

1 Pointwise distance distributions of periodic sets

2 Daniel Widdowson ✉ 

3 Department of Computer Science, University of Liverpool, Liverpool, United Kingdom

4 Vitaliy Kurlin ✉ 

5 Department of Computer Science, University of Liverpool, Liverpool, United Kingdom

6 — Abstract —

7 The fundamental model of a periodic structure is a periodic set of points considered up to rigid
8 motion or isometry in Euclidean space. The recent work by Edelsbrunner et al defined the new
9 isometry invariants (density functions), which are continuous under perturbations of points and
10 complete for generic sets in dimension 3. This work introduces much faster invariants called higher
11 order Pointwise Distance Distributions (PDD). The new PDD invariants are simpler represented
12 by numerical matrices and are also continuous under perturbations important for applications.
13 Completeness of PDD invariants is proved for distance-generic sets in any dimension, which was also
14 confirmed by distinguishing all 229K known molecular organic structures from the world's largest
15 Cambridge Structural Database. This huge experiment took only seven hours on a modest desktop
16 due to the proposed algorithm with a near linear or small polynomial complexity in terms of key
17 input sizes. Most importantly, the above completeness allows one to build a common map of all
18 periodic structures, which are continuously parameterized by PDD and explicitly reconstructible
19 from PDD. Appendices include first tree-based maps for several thousands of real structures.

20 **2012 ACM Subject Classification** Theory of computation → Computational geometry

21 **Keywords and phrases** Lattices, periodic sets, isometry invariants, continuity, complete classification

22 **Funding** *Vitaliy Kurlin*: EPSRC grant ‘Application-driven Topological Data Analysis’, EP/R018472/1

1 Motivations, problem statement and overview of new results

This paper develops polynomial time algorithms for new invariants of discrete structures, which allow one to distinguish and visualize largest datasets of real periodic structures.

The recent work by Edelsbrunner et al [18] initiated a new direction in classifications of periodic point sets up to isometry. An *isometry* of Euclidean space \mathbb{R}^n is any map that preserves inter-point distances. Any orientation-preserving isometry can be realised as a continuous rigid motion, for example any composition of translations and rotations in \mathbb{R}^3 . This equivalence is most natural for periodic point sets that represent real rigid structures.

A *lattice* Λ consists of all integer linear combinations of a basis whose vectors span a parallelepiped called a *unit cell* U . A *periodic point set* is the Minkowski sum $\Lambda + M = \{\vec{u} + \vec{v} : u \in \Lambda, v \in M\}$, where a *motif* M is a finite set of points in the basis of U [45].

A real periodic structure such as a solid crystalline material is best modeled as a periodic set $S \subset \mathbb{R}^n$ of points at all atomic centers, whose positions have a physical meaning and are well-determined by X-ray diffraction. Chemical bonds between atoms only abstractly represent atomic interactions depending on many thresholds for distances and angles.

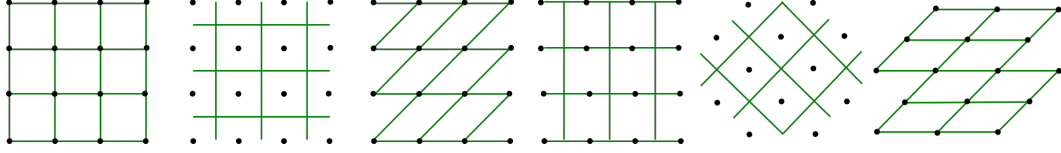


Figure 1 Six lattices are defined by different cells and motifs but are isometric to each other. **1st:** $U = \langle(1, 0), (0, 1)\rangle$ and $M = \{(0, 0)\}$. **2nd:** $U = \langle(1, 0), (0, 1)\rangle$ and $M = \{(\frac{1}{2}, \frac{1}{2})\}$. **3rd:** $U = \langle(1, 0), (1, 1)\rangle$ and $M = \{(0, 0)\}$. **4th:** $U = \langle(1, 0), (0, 1)\rangle$ and $M = \{(\frac{1}{2}, 0)\}$. **5th:** $U = \langle(\frac{1}{\sqrt{2}}, \frac{1}{\sqrt{2}}), (-\frac{1}{\sqrt{2}}, \frac{1}{\sqrt{2}})\rangle$ and $M = \{(\frac{1}{2}, \frac{1}{2})\}$. **6th:** $U = \langle(\sqrt{2}, 0), (\frac{1}{\sqrt{2}}, \frac{1}{\sqrt{2}})\rangle$ and $M = \{(0, 0)\}$.

Fig. 1 illustrates the first obstacle: the same lattice can be generated by infinitely many different bases or unit cells. So distinguishing lattices up to isometry is already non-trivial.

Fig. 2 shows that ambiguity of a conventional representation $S = \Lambda + M$ for periodic structures by a unit cell and a motif M is actually deeper than the case of only lattices.

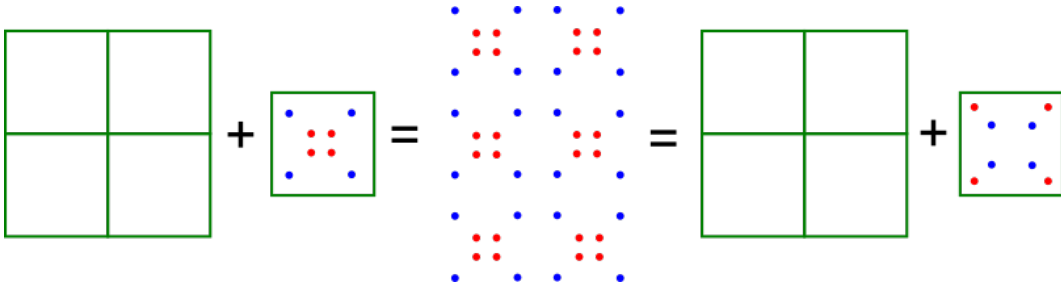
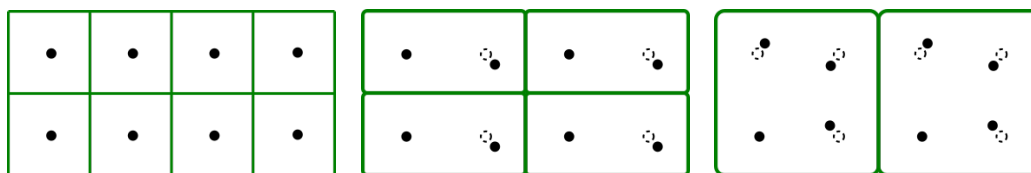


Figure 2 Even for a fixed lattice Λ , different motifs M can define isometric periodic sets $\Lambda + M$.

Periodic structures can be reliably distinguished up to isometry only by an isometry invariant that takes the same value for all isometric sets. We include mirror reflections into general isometries only for simplicity, because adding a sign of orientation to any isometry invariant can be straightforward. Non-invariants such as edge-lengths and angles of a unit cell, or coordinates of motif point in a cell basis cannot be used for an isometry classification. Indeed, isometric sets can have different values of a non-invariant, see Fig. 1 and 2.

48 The traditional approach is to identify a crystal by using its conventional or reduced
 49 cell [23, section 9.3]. However, this reduced cell has been known to be discontinuous under
 50 perturbations [3] even for lattices when a motif M is a single point. A continuous reduced
 51 cell of a lattice cannot exist, see [18, section 1].

52 For more general periodic sets, discontinuity of many past discrete invariants such as
 53 symmetry groups is clearer in Fig. 3 showing that even real-valued invariants struggle to
 54 continuously quantify a similarity between nearly identical periodic sets. For example, the
 55 minimal volume of any cell can easily double, while the density (the number or mass of
 56 points divided by the cell volume) remains constant under perturbations of points. Hence a
 57 continuous isometry classification of periodic point sets has been open at least since 1980 [3].



■ **Figure 3** Under almost any slight perturbation of points, the symmetry group and (the minimum volume of) any reduced cell discontinuously change, which justifies condition (1c) in Problem 1.

58 Continuity is practically important because atoms always vibrate above the absolute zero
 59 temperature. Any real measurement of atomic positions produces slightly different parameters
 60 of a unit cell and a motif. Any simulation of periodic structures similarly introduces floating
 61 point errors because of inevitable approximations in all iterative optimizations.

62 Thousands of near duplicates are routinely produced, though only a few structures are
 63 synthesized. Five real structures of 5679 predicted on a supercomputer over 12 weeks are a
 64 typical example [35]. This ‘embarrassment of over-prediction’ wastes resources and time to
 65 run simulations and then to analyze results, often by visual inspection, because there were
 66 no fast and reliable tools to quantify a similarity between periodic structures.

67 One natural similarity measure is the maximum displacement atoms under thermal
 68 vibrations. This *bottleneck distance* $d_B(S, Q)$ between periodic point sets is the maximum
 69 Euclidean distance needed to perturb every point $p \in S$ to its unique match in Q . Since d_B
 70 is minimized over infinitely many bijections and points, d_B is computationally intractable.

71 Continuity of isometry invariants can be measured with respect to the bottleneck distance
 72 d_B . The polynomial time (P) is relative to the number of motif points for a fixed dimension.

- 73 ► **Problem 1** (algorithmic classification). Find a function I on periodic point sets such that
 74 (1a) *invariance* : if $S, Q \subset \mathbb{R}^n$ are isometric, then $I(S) = I(Q)$, which is checked in P time;
 75 (1b) *computability* : a distance d between values of an invariant I is computable in P time;
 76 (1c) *Lipschitz continuity* : $d(I(S), I(Q)) \leq C d_B(S, Q)$ for a constant C and $S, Q \subset \mathbb{R}^n$;
 77 (1d) *completeness* : if $I(S) = I(Q)$ for periodic point sets S, Q , then S, Q are isometric;
 78 (1e) *reconstruction* : any periodic point set $S \subset \mathbb{R}^n$ can be reconstructed from $I(S)$. ■

79 The proposed invariant is the higher order Pointwise Distance Distribution $\text{PDD}^{\{h\}}$.
 80 The first order PDD was studied only for finite sets [29] and is now proved to satisfy all
 81 conditions of Problem 1 except possibly (1d). Completeness of PDD is proved in Theorem 9
 82 for distance-generic sets approximating all periodic sets and is experimentally checked for all
 83 known 229K organic crystals from the world’s largest Cambridge Structural Database, which
 84 puts them all onto a common map continuously extending the periodic table of elements.

2 Definitions and a review of past work on comparing periodic sets

This section rigorously defines periodic point sets, which cannot be reconstructed from their finite subsets in Fig. 4 without a lattice basis whose discontinuity was a major obstacle.

Any point p in \mathbb{R}^n can be identified with the vector \vec{p} from the origin 0 to p . The Euclidean distance between $p, q \in \mathbb{R}^n$ is denoted by $|p - q|$, which is the length of $\vec{p} - \vec{q}$.

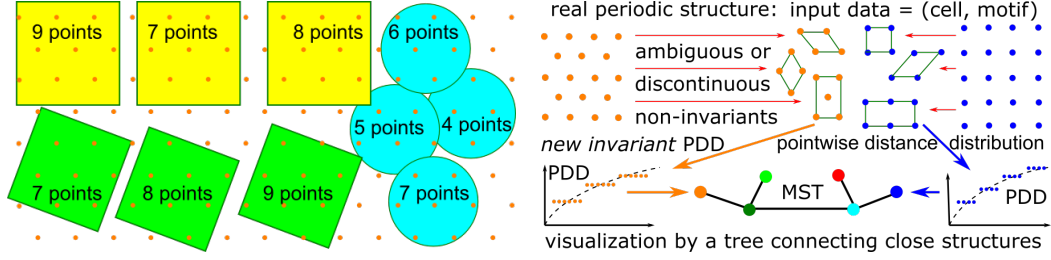


Figure 4 Left: hard to choose a finite subset that truly represents an infinite periodic set, discontinuity under perturbations of points or set sizes is similar to Fig. 3. Right: ambiguous input is transformed into the invariant PDD to visualize any real dataset as a Minimum Spanning Tree.

Definition 2 (a lattice Λ , a motif M , a periodic point set $S = \Lambda + M$). A lattice Λ in \mathbb{R}^n consists of all linear combinations $\sum_{i=1}^n c_i \vec{v}_i$ with $c_i \in \mathbb{Z}$. The vectors $\vec{v}_1, \dots, \vec{v}_n$ should form a basis so that if $\sum_{i=1}^n c_i \vec{v}_i = \vec{0}$ for some c_i , then all $c_i = 0$. A motif M is a finite set of points p_1, \dots, p_m in the unit cell $U(\vec{v}_1, \dots, \vec{v}_n) = \left\{ \sum_{i=1}^n c_i \vec{v}_i : c_i \in [0, 1) \right\}$, which is the parallelepiped spanned by $\vec{v}_1, \dots, \vec{v}_n$. A periodic point set $S \subset \mathbb{R}^n$ is the Minkowski sum of a lattice Λ and a motif M , so $S = \Lambda + M = \{ \vec{u} + \vec{v} : u \in \Lambda, v \in M \}$. A unit cell U is primitive if S is invariant under shifts by only $\vec{v} \in \Lambda$ that is generated by vectors along edges of U . ■

Any lattice Λ is considered as a periodic set with a 1-point motif $M = \{p\}$. A single point p can be arbitrarily chosen in a unit cell U as in the first two pictures of Fig. 1. Notice that the U is half-open in the sense that coefficients $\lambda_i \in [0, 1)$ can take value 0, but not 1.

Now we discuss the closely related work on comparing finite and periodic sets up to isometry. The excellent book [25] reviews the wider area of Euclidean distance geometry.

For a finite set $S \subset \mathbb{R}^n$, the distribution of all pairwise is a complete invariant in general position [9] meaning that almost any finite set can be uniquely reconstructed up to isometry from the set of all pairwise distances. The non-isometric 4-point sets in Figure 5 are a classical counter-example to the completeness of this distribution of all pairwise distances.

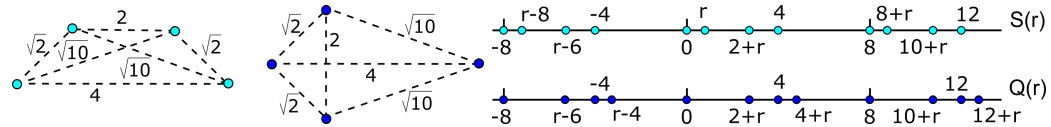


Figure 5 Left: point sets $K = \{(\pm 2, 0), (\pm 1, 1)\}$ and $T = \{(\pm 2, 0), (-1, \pm 1)\}$ can not be distinguished by their six pairwise distances $\sqrt{2}, \sqrt{2}, \sqrt{10}, \sqrt{10}, 4$. Right: 1D periodic sets $S(r) = \{0, r, 2+r, 4\} + 8\mathbb{Z}$ and $Q(r) = \{0, 2+r, 4, 4+r\} + 8\mathbb{Z}$ for $0 < r \leq 1$ have the same Patterson function [31, p. 197, Fig. 2]. All these pairs are distinguished by the first order PDD in section 3.

106 The isometry classification of finite point sets was algorithmically resolved by Theorem 1
 107 in [2] saying that the existence of an isometry between two m -point sets in \mathbb{R}^n can be checked
 108 in time $O(m^{n-2} \log m)$. The latest advance for finite sets is the $O(m \log m)$ algorithm in \mathbb{R}^4
 109 [24]. Significant results on matching bounded rigid shapes and registration of finite point
 110 sets were obtained in [38, 44, 27, 17]. The research on graph isomorphisms [40, 1] can be
 111 potentially used for periodic graphs with fixed edges between points of a periodic set.

112 Mémoli's seminal work on *distributions of distances* [29], also known as *shape distributions*
 113 [30, 6, 21, 26, 32], for bounded metric spaces is closest to the proposed Pointwise Distance
 114 Distributions (PDD) for periodic point sets. In addition to periodicity not reducible to a
 115 bounded case, see Fig. 4, another crucial novelty is the higher order extension $\text{PDD}^{\{h\}}$ in
 116 Definition 4 capturing the isometry information of $(h+1)$ -point tuples beyond the case $h=1$
 117 of pairs. Continuity of distance distributions was not yet addressed but is essential to filter
 118 out near duplicates among thousands or even millions of simulated structures [35].

119 The latest breakthrough in fast comparisons of probability measures [39] can help speed
 120 up computations of Earth Mover's Distance (EMD), which will be proved to be continuous
 121 for Pointwise Distance Distributions $\text{PDD}^{\{h\}}$. The discontinuity under perturbations of
 122 points is the major weakness of all discrete invariants including symmetry groups and other
 123 group-theoretic invariants of periodic point sets [20]. The two nearly identical periodic sets
 124 in Figure 3 should be recognized as very similar. But they have different symmetries and
 125 can be related only by pseudo-symmetries depending on manual thresholds [46].

126 One of the oldest crystal structure descriptors is the X-ray diffraction pattern whose single
 127 crystal form is best for determining a 3D structure of an experimental crystal [14]. Since not
 128 all materials can be grown as single crystals, the powder X-ray diffraction pattern (PXRD)
 129 is more common. Periodic structures with identical PXRDs are called *homometric*, [36], for
 130 example the periodic versions $S(1) = \{0, 1, 3, 4\} + 8\mathbb{Z}$ and $Q(1) = \{0, 3, 4, 5\} + 8\mathbb{Z}$ of the
 131 4-point non-isometric sets T, K in Fig. 5. Even more general homometric sets $S(r), Q(r)$
 132 depending on a $0 < r \leq 1$ will be distinguished by the first order PDD in section 3.

133 The Mercury software visually compares periodic structures [11] by minimizing the Root
 134 Mean Square Deviation (RMSD) of atomic positions from up to a given number m (15 by
 135 default) of molecules in two structures. This RMSD measures a similarity between only finite
 136 subsets as in Fig. 4 and will be compared with the new PDD invariants in section 6.

137 More recently, for any periodic point set $S \subset \mathbb{R}^n$ with a motif M in a unit cell U ,
 138 Edelsbrunner et al. [18] introduced the density functions $\psi_k(t)$ for any integer $k \geq 1$. The
 139 k -th *density function* $\psi_k(t)$ is the total volume of the regions within the unit cell U covered
 140 by exactly k balls $B(p; t)$ with a radius $t \geq 0$ and centres at points $p \in M$, divided by the unit
 141 cell volume $\text{Vol}[U]$. The density function $\psi_k(t)$ was proved to be invariant under isometry,
 142 continuous under perturbations, complete for periodic sets satisfying certain conditions of
 143 general position in \mathbb{R}^3 , and computable in time $O(mk^3)$, where m is the motif size of S .

144 Section 5 in [18] gives the counter-example to completeness: the 1-dimensional periodic
 145 sets $S_{15} = X + Y + 15\mathbb{Z}$ and $Q_{15} = X - Y + 15\mathbb{Z}$ for $X = \{0, 4, 9\}$ and $Y = \{0, 1, 3\}$, which
 146 appeared earlier in [22, section 4]. These non-isometric sets have the same density functions
 147 for all $k \geq 1$, see [4, Example 11], and were recently distinguished in [43, Example 5b].

148 The latest advance [5] reduces the isometry classification of all periodic point sets to an
 149 *isoset* of isometry classes of α -clusters around points in a motif at a certain radius α , which
 150 was motivated by the seminal work of Dolbilin with co-authors about Delone sets [16, 8, 15].
 151 Checking if two isosets coincide needs a cubic algorithm, which is not yet implemented.

152 **3 The higher order Pointwise Distance Distributions** $\text{PDD}^{\{h\}}(S; k)$

153 This section introduces the Pointwise Distance Distributions PDD in Definition 3 and the
 154 higher order $\text{PDD}^{\{h\}}$ in Definition 4, whose isometry invariance is proved by Theorem 5.

155 For periodic point sets, distances to neighbors were considered in [43, Definition 5],
 156 though only their average was proved to be invariant under permutations of points. Moreover,
 157 doubling a unit cell and perturbing points as in Fig. 3 produces a twice larger list of distances.
 158 New Definition 3 below introduces weights that make PDD continuous under perturbations
 159 in Theorem 7. We consider only periodic point sets, though the lexicographic ordering of
 160 rows in PDD makes it invariant for any finite set of weighted points in a metric space.

161 **► Definition 3** (Pointwise Distance Distribution PDD). Let a periodic set $S = \Lambda + M$ have
 162 points p_1, \dots, p_m in a unit cell. For $k \geq 1$, consider the $m \times k$ matrix $D(S; k)$, whose i -th
 163 row consists of the ordered Euclidean distances $d_{i1} \leq \dots \leq d_{ik}$ measured from p_i to its
 164 first k nearest neighbors in the full set S . The rows of $D(S; k)$ are *lexicographically* ordered
 165 as follows. A row (d_{i1}, \dots, d_{ik}) is *smaller* than (d_{j1}, \dots, d_{jk}) if the first (possibly none)
 166 distances coincide: $d_{i1} = d_{j1}, \dots, d_{il} = d_{jl}$ for $l \in \{1, \dots, k-1\}$ and the next $(l+1)$ -st
 167 distances satisfy $d_{i,l+1} < d_{j,l+1}$. If w rows are identical to each other, any such group is
 168 collapsed to a single row with the *weight* w/m . For each row, put this weight in the first
 169 column. The final $m \times (k+1)$ -matrix is the *Pointwise Distance Distribution* $\text{PDD}(S; k)$. ■

170 Table 1 shows the 4×3 matrices $D(S; 3)$ from Definition 3 for the 4-point sets in Fig. 5. The
 171 matrix $D(T; 3)$ in Table 1 has two pairs of identical rows, so the matrix $\text{PDD}(T; 3)$ consists
 172 of two rows of weight $\frac{1}{2}$ below. The matrix $D(K; 3)$ in Table 1 has only one pair of identical
 173 rows, so $\text{PDD}(K; 3)$ has three rows of weights $\frac{1}{2}, \frac{1}{4}, \frac{1}{4}$. Then $\text{PDD}(T; 3) \neq \text{PDD}(K; 3)$

T points	neighb.1	neighb.2	neighb.3	K points	neighb.1	neighb.2	neighb.3
$(-2, 0)$	$\sqrt{2}$	$\sqrt{10}$	4	$(-2, 0)$	$\sqrt{2}$	$\sqrt{2}$	4
$(+2, 0)$	$\sqrt{2}$	$\sqrt{10}$	4	$(+2, 0)$	$\sqrt{10}$	$\sqrt{10}$	4
$(-1, 1)$	$\sqrt{2}$	2	$\sqrt{10}$	$(-1, -1)$	$\sqrt{2}$	2	$\sqrt{10}$
$(+1, 1)$	$\sqrt{2}$	2	$\sqrt{10}$	$(-1, +1)$	$\sqrt{2}$	2	$\sqrt{10}$

■ **Table 1** Each point in $T, K \subset \mathbb{R}^2$ from Figure 5 has ordered distances to three other points.

174
$$\text{PDD}(T; 3) = \left(\begin{array}{c|ccc} 1/2 & \sqrt{2} & 2 & \sqrt{10} \\ 1/2 & \sqrt{2} & \sqrt{10} & 4 \end{array} \right) \neq \text{PDD}(K; 3) = \left(\begin{array}{c|ccc} 1/4 & \sqrt{2} & \sqrt{2} & 4 \\ 1/2 & \sqrt{2} & 2 & \sqrt{10} \\ 1/4 & \sqrt{10} & \sqrt{10} & 4 \end{array} \right).$$

$S(r)$ points	distance to neighbor 1	distance to neighbor 2	distance to neighbor 3
$p_1 = 0$	$ 0 - r = r$	$ 0 - (2 + r) = 2 + r$	$ 0 - 4 = 4$
$p_2 = r$	$ r - 0 = r$	$ r - (2 + r) = 2$	$ r - 4 = 4 - r$
$p_3 = 2 + r$	$ (2 + r) - 4 = 2 - r$	$ (2 + r) - r = 2$	$ (2 + r) - 0 = 2 + r$
$p_4 = 4$	$ 4 - (2 + r) = 2 - r$	$ 4 - r = 4 - r$	$ 4 - 0 = 4$
$Q(r)$ points	distance to neighbor 1	distance to neighbor 2	distance to neighbor 3
$p_1 = 0$	$ 0 - (2 + r) = 2 + r$	$ 0 - (r + 4 - 8) = 4 - r$	$ 0 - 4 = 4$
$p_2 = 2 + r$	$ (2 + r) - 4 = 2 - r$	$ (2 + r) - (4 + r) = 2$	$ (2 + r) - 0 = 2 + r$
$p_3 = 4$	$ 4 - (4 + r) = r$	$ 4 - (2 + r) = 2 - r$	$ 4 - 0 = 4$
$p_4 = 4 + r$	$ (4 + r) - 4 = r$	$ (4 + r) - (2 + r) = 2$	$ (4 + r) - 8 = 4 - r$

■ **Table 2** Distances from each motif point of $S(r)$ and $Q(r)$ to their closest neighbors in Fig. 5.

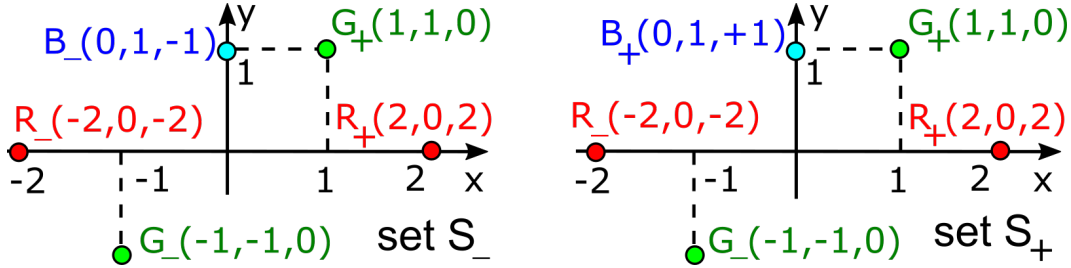
For the 1D periodic sets $S(r) = \{0, r, 2 + r, 4\} + 8\mathbb{Z}$ and $Q(r) = \{0, 2 + r, 4, 4 + r\} + 8\mathbb{Z}$ in Fig. 5, Table 2 shows that $S(r), Q(r)$ are not isometric to each other for any parameter $0 < r < 1$ due to Invariance Theorem 5 stated later for higher order $\text{PDD}^{\{h\}}$.

$$\text{PDD}(S(r); 2) = \begin{pmatrix} 1/4 & r & 2+r \\ 1/4 & r & 2 \\ 1/4 & 2-r & 2 \\ 1/4 & 2-r & 4-r \end{pmatrix} \neq \text{PDD}(Q(r); 2) = \begin{pmatrix} 1/4 & r & 2-r \\ 1/4 & r & 2 \\ 1/4 & 2-r & 2 \\ 1/4 & 2+r & 4-r \end{pmatrix}.$$

175 The Average Minimum Distance $\text{AMD}_k(S)$ from [43, Definition 5] is the average of the
 176 $(k+1)$ -st column of $\text{PDD}(S; k)$. The vectors $\text{AMD}(S(r); 6) = (1, 2.5, 3.5)$ don't distinguish
 177 the sets $S(r)$ in Fig. 5. Hence $\text{PDD}(S; k)$ is strictly stronger than $\text{AMD}(S; k)$.

178 For a periodic set S , the number k in $\text{PDD}(S; k)$ can be considered as a degree of
 179 approximation (or a count of decimal places), not as not a parameter that affects invariant
 180 values. If we increase k , we extract more distant geometric information from S by add more
 181 columns to $\text{PDD}(S; k)$ and keep all previous distances. If some rows of $\text{PDD}(S; k-1)$ were
 182 identical but become different in $\text{PDD}(S; k)$, we recompute weights but not distances.

183 Fig. 6 shows the 5-point sets $S_{\pm} \subset \mathbb{R}^3$ from [33, Figure S4(A)], which were considered
 184 as a hard pair to distinguish. The sets S_{\pm} are not isometric, because S_+ has the triple of
 185 points $B_+G_+R_+$ with pairwise distances $\sqrt{2}, \sqrt{6}, \sqrt{6}$, but S_- has no such a triple. This
 186 example motivated our stronger invariant. Instead of collecting triples of distances, we extend
 187 Definition 3 to represent relations between h -tuples for $h > 1$ in a matrix form.



188 **Figure 6 Left:** (x, y) -projection of the 5-point set $S_- \subset \mathbb{R}^3$ consisting of the green points
 189 $G_- = (-1, -1, 0)$ and $G_+ = (1, 1, 0)$, the red points $R_- = (-2, 0, -2)$ and $R_+ = (2, 0, 2)$, and the
 blue point $B_- = (0, 1, -1)$. **Right:** to get the set $S_+ \subset \mathbb{R}^3$ from S_- , replace B_- by $B_+ = (0, 1, 1)$.

188 **Definition 4** (higher order Pointwise Distance Distribution $\text{PDD}^{\{h\}}(S; k)$). Let a periodic
 189 set $S = \Lambda + M$ have points p_1, \dots, p_m in its motif M . We start from the case $h = 2$.

190 For any $k \geq 1$, we build the $\frac{m(m-1)}{2} \times (k+2)$ matrix $\text{PDD}^{\{2\}}(S)$. For each unordered
 191 pair $\{p_i, p_j\}$ of distinct points with $i \neq j$, construct the row whose first element is the distance
 192 $|\vec{p}_i - \vec{p}_j|$ and every element is the ordered pair of distances $|\vec{p}_i - \vec{p}_l|, |\vec{p}_j - \vec{p}_l|$ to another point
 193 p_l for $l \neq i, j$, i.e. in each pair the first distance is not smaller than the second. In every
 194 row these pairs are lexicographically ordered, i.e. $(a, b) < (c, d)$ if $a < c$ or $a = c, b < d$.
 195 Table 6 includes the first column with pairs $\{p_i, p_j\}$ for convenience. To avoid a dependence
 196 on any ordering of p_1, \dots, p_m , we remove this first column and order the resulting rows
 197 lexicographically, we compare distances $|\vec{p}_i - \vec{p}_j|$ and then (in the case of equal distances) we
 198 compare the ordered pairs of distances. We collapse all rows that are identical to each other
 199 and put weights into the first column as in Definition 3, see Table 3 for S_{\mp} in Fig. 6.

S_{\pm} : weight	dist.	dist.pair to neighbor 1	dist.pair to neighbor 2	dist.pair to neighbor 3
1/10	$\sqrt{2}$	$(\sqrt{6}, \sqrt{8})$	$(\sqrt{6}, \sqrt{14})$	$(\sqrt{6}, \sqrt{14})$
1/10	$\sqrt{6}$	$(\sqrt{2}, \sqrt{8})$	$(\sqrt{6}, \sqrt{6})$	$(\sqrt{14}, \sqrt{14})$
1/10	$\sqrt{6}$	$(\sqrt{2}, \sqrt{14})$	$(\sqrt{6}, \sqrt{6})$	$(\sqrt{14}, \sqrt{32})$
1/10	$\sqrt{6}$	$(\sqrt{2}, \sqrt{14})$	$(\sqrt{8}, \sqrt{14})$	$(\sqrt{14}, \sqrt{32})$
1/10	$\sqrt{6}$	$(\sqrt{6}, \sqrt{6})$	$(\sqrt{8}, \sqrt{14})$	$(\sqrt{14}, \sqrt{32})$
1/10	$\sqrt{8}$	$(\sqrt{2}, \sqrt{6})$	$(\sqrt{6}, \sqrt{14})$	$(\sqrt{6}, \sqrt{14})$
1/10	$\sqrt{14}$	$(\sqrt{2}, \sqrt{6})$	$(\sqrt{6}, \sqrt{8})$	$(\sqrt{6}, \sqrt{32})$
1/10	$\sqrt{14}$	$(\sqrt{2}, \sqrt{6})$	$(\sqrt{6}, \sqrt{14})$	$(\sqrt{6}, \sqrt{32})$
1/10	$\sqrt{14}$	$(\sqrt{6}, \sqrt{8})$	$(\sqrt{6}, \sqrt{14})$	$(\sqrt{6}, \sqrt{32})$
1/10	$\sqrt{32}$	$(\sqrt{6}, \sqrt{14})$	$(\sqrt{6}, \sqrt{14})$	$(\sqrt{6}, \sqrt{14})$

S_{\pm} : weight	dist.	dist.pair to neighbor 1	dist.pair to neighbor 2	dist.pair to neighbor 3
1/10	$\sqrt{2}$	$(\sqrt{6}, \sqrt{6})$	$(\sqrt{6}, \sqrt{8})$	$(\sqrt{14}, \sqrt{14})$
1/10	$\sqrt{6}$	$(\sqrt{2}, \sqrt{6})$	$(\sqrt{6}, \sqrt{14})$	$(\sqrt{14}, \sqrt{32})$
1/10	$\sqrt{6}$	$(\sqrt{2}, \sqrt{6})$	$(\sqrt{8}, \sqrt{14})$	$(\sqrt{14}, \sqrt{32})$
1/10	$\sqrt{6}$	$(\sqrt{2}, \sqrt{8})$	$(\sqrt{6}, \sqrt{14})$	$(\sqrt{6}, \sqrt{14})$
1/10	$\sqrt{6}$	$(\sqrt{6}, \sqrt{14})$	$(\sqrt{8}, \sqrt{14})$	$(\sqrt{14}, \sqrt{32})$
1/10	$\sqrt{8}$	$(\sqrt{2}, \sqrt{6})$	$(\sqrt{6}, \sqrt{14})$	$(\sqrt{6}, \sqrt{14})$
1/10	$\sqrt{14}$	$(\sqrt{2}, \sqrt{14})$	$(\sqrt{6}, \sqrt{6})$	$(\sqrt{6}, \sqrt{32})$
1/10	$\sqrt{14}$	$(\sqrt{2}, \sqrt{14})$	$(\sqrt{6}, \sqrt{8})$	$(\sqrt{6}, \sqrt{32})$
1/10	$\sqrt{14}$	$(\sqrt{6}, \sqrt{6})$	$(\sqrt{6}, \sqrt{8})$	$(\sqrt{6}, \sqrt{32})$
1/10	$\sqrt{32}$	$(\sqrt{6}, \sqrt{14})$	$(\sqrt{6}, \sqrt{14})$	$(\sqrt{6}, \sqrt{14})$

■ **Table 3** The 2nd order Pointwise Distance Distribution $\text{PDD}^{\{2\}}(S_{\pm})$ is obtained by lexicographically ordering the rows of Table 6 and replacing pairs of points in column 1 by weights of rows.

200 For $h > 2$, each row of $\text{PDD}^{\{h\}}(S; k)$ has data related to an unordered subset $A \subset S$ of h
 201 points. In each row, the first element is the weight coming from collapsing identical rows in
 202 the final matrix $\text{PDD}^{\{h\}}(S; k)$ as for $h = 1$. The second element is the $h \times (h - 1)$ matrix
 203 $D(A; h - 1)$, whose every row has ordered distances from $p \in A$ to all other $h - 1$ points in A ,
 204 all rows are lexicographically ordered. Other elements of $\text{PDD}^{\{h\}}(S; k)$ are lexicographically
 205 ordered lists of distances $d_{i1} \leq \dots \leq d_{ih}$ from a point $p_i \in S - A$ to the h points of A . ■

206 Definition 4 makes sense for a finite set S of m points, then $k \leq m - 1$. Similarly to
 207 Definition 4, increasing an index $k \geq 1$ only adds more information about S without changing
 208 values obtained for smaller k . Similarly the order h is not a parameter that affects values of
 209 $\text{PDD}^{\{h\}}(S; k)$, because all $\text{PDD}^{\{h\}}(S; k)$ are different matrices for distinct orders h .

210 Already the second order $\text{PDD}^{\{2\}}$ distinguishes non-isometric sets that have identical
 211 invariants from [33, section 6 in supplementary materials]. The 5-point sets S_{\pm} in Fig. 6
 212 have $\text{PDD}^{\{2\}}(S_-) \neq \text{PDD}^{\{2\}}(S_+)$. The pairs in Table 3 represent G_+B_{\mp} , which have the
 213 same shortest distance $\sqrt{2}$ in both S_{\mp} but the distinct pairs of distances to the first neighbor:
 214 $(\sqrt{6}, \sqrt{8})$ from (G_+, B_-) to G_- , $(\sqrt{6}, \sqrt{6})$ from (G_+, B_+) to R_+ , see details in appendix C.

215 We have chosen only distances to form the stronger higher order invariant $\text{PDD}^{\{h\}}$, not
 216 angles or other isometry invariants such as volumes, because distances are simple enough to
 217 prove the continuity of $\text{PDD}^{\{h\}}$ under perturbations of points in Theorem 7 later.

218 ► **Theorem 5** (isometry invariance of $\text{PDD}^h(S; k)$). *For any finite or periodic set $S \subset \mathbb{R}^n$,*
 219 *$\text{PDD}^{\{h\}}(S; k)$ from Definition 3 is an isometry invariant of the set S for any $k \geq 1$.* ■

220 *Short proof.* Any isometry preserves inter-point distances, see details in Appendix B. \square

221 **4 Continuity of Pointwise Distance Distributions under perturbations**

222 Definition 6 below works for any vector $I(S) = ([w_1(S), R_1(S)], \dots, [w_{n(S)}(S), R_{n(S)}(S)])$ of
 223 pointwise invariants of a set S with weights $w_i(S) \in (0, 1]$ satisfying $\sum_{i=1}^{n(S)} w_i(S) = 1$.

224 Later we consider only the case when $[w_i, R_i]$ is the i -th row of $\text{PDD}^{\{h\}}(S; k)$. Then $n(S)$
 225 is the number of rows in $\text{PDD}^{\{h\}}(S; k)$. Each component $R_i(S)$ should have a size independent
 226 of S , for example a number k of neighbors in $\text{PDD}(S; k)$. For $h > 1$, the index i represents
 227 an unordered subset $A \subset S$ of h points. The first component of R_i is the $h \times (h - 1)$ matrix
 228 $D(A)$ of ordered distance lists from Definition 4. For any vectors $R_i = (r_{i1}, \dots, r_{ik})$ and
 229 $R_j = (r_{j1}, \dots, r_{jk})$ of a length k , we use the L_∞ -distance $|R_i - R_j|_\infty = \max_{l=1, \dots, k} |r_{il} - r_{jl}|_\infty$,
 230 where $|r_{il} - r_{jl}|_\infty$ is again the L_∞ -distance between the components r_{il}, r_{jl} (Euclidean
 231 distance if r_{il}, r_{jl} are single numbers). For $h > 1$, the first component r_{i1} of R_i is the matrix
 232 $D(A; h - 1)$ for a subset $A_i \subset S$ of h points. To get $|r_{i1} - r_{j1}|_\infty$, we turn the matrices
 233 $D(A_i; h - 1), D(B_j; h - 1)$ into vectors by concatenating all rows.

234 **► Definition 6 (EMD).** Let finite or periodic sets $S, Q \subset \mathbb{R}^n$ have weighted vectors $I(S), I(Q)$
 235 as discussed above. A full *flow* from $I(S)$ to $I(Q)$ is an $m(S) \times m(Q)$ matrix whose element
 236 $f_{ij} \in [0, 1]$ represents a partial *flow* from $R_i(S)$ to $R_j(Q)$. The *Earth Mover's Distance* is the
 237 minimum value of $\text{EMD}(I(S), I(Q)) = \sum_{i=1}^{m(S)} \sum_{j=1}^{m(Q)} f_{ij} |R_i(S) - R_j(Q)|$ over $f_{ij} \in [0, 1]$ subject
 238 to $\sum_{j=1}^{m(Q)} f_{ij} \leq w_i$ for $i = 1, \dots, m(S)$, $\sum_{i=1}^{m(S)} f_{ij} \leq u_j$ for $j = 1, \dots, m(Q)$, $\sum_{i=1}^{m(S)} \sum_{j=1}^{m(Q)} f_{ij} = 1$. \blacksquare

239 The first condition $\sum_{j=1}^{m(Q)} f_{ij} \leq w_i(S)$ means that not more than the weight $w_i(S)$ of
 240 the component $R_i(S)$ ‘flows’ into all components $R_j(Q)$ via ‘flows’ f_{ij} , $j = 1, \dots, m(Q)$.
 241 Similarly, the second condition $\sum_{i=1}^{m(S)} f_{ij} = w_j(Q)$ means that all ‘flows’ f_{ij} from $R_i(S)$ for
 242 $i = 1, \dots, m(S)$ ‘flow’ into $R_j(Q)$ up to the maximum weight $w_j(Q)$. The last condition
 243 $\sum_{i=1}^{m(S)} \sum_{j=1}^{m(Q)} f_{ij} = 1$ forces to ‘flow’ all rows $R_i(S)$ into all rows $R_j(Q)$. The Earth Mover’s
 244 Distance satisfies all metric axioms [37, appendix]. The EMD needs $O(m^3 \log m)$ time for
 245 distributions of a maximum size m or can be approximated in a time $O(m)$ [41].

246 Theorem 7 uses the bottleneck distance $d_B(S, Q) = \inf_{g: S \rightarrow Q} \sup_{p \in S} |p - g(p)|$ and the *packing*
 247 *radius* $r(S)$, which is the minimum half-distance between any points of S . Equivalently, $r(S)$
 248 is the maximum radius r to have disjoint open balls of radius r centered at all points of S .

249 **► Theorem 7 (continuity of $\text{PDD}^{\{h\}}$).** For any $k \geq 1$, if finite or periodic sets $S, Q \subset \mathbb{R}^n$
 250 satisfy $d_B(S, Q) < r(S)$, then $\text{EMD}(\text{PDD}^{\{h\}}(S; k), \text{PDD}^{\{h\}}(Q; k)) \leq 2d_B(S, Q)$. \blacksquare

251 *Short proof.* If any point of S is perturbed up to $\varepsilon = d_B(S, Q)$ to match a unique point of Q ,
 252 then each row in $\text{PDD}(S; k)$ of ordered distances from a point $p \in S$ changes up to 2ε in the
 253 L_∞ -distance, which leads to factor 2 in estimating EMD, see details in Appendix B. \square

5 Generic completeness of Pointwise Distance Distributions

Following the earlier work [18, section 5.1], this section defines distance-generic periodic point sets that can be uniquely reconstructed up to isometry from first order Pointwise Distance Distributions in dimension $n = 2$. For $n = 3$, we will also use conorms p_{ij} of a lattice [12], which are continuous isometry invariants expressed via scalar products of basis vectors.

Any lattice $\Lambda \subset \mathbb{R}^n$ in dimensions $n \leq 3$ has an obtuse superbase $\vec{v}_1, \dots, \vec{v}_n$ with the extra $\vec{v}_0 = -\sum_{i=1}^n \vec{v}_i$ such that $p_{ij} = -\vec{v}_i \cdot \vec{v}_j \geq 0$ for distinct $i, j = 0, \dots, n$. These negative Selling parameters were called *conorms* of Λ in [12], where formula (1) for p_{ij} missed the minus, but the rest of the paper needs $p_{ij} \geq 0$, for example in Selling's formula (5).

For any lattice $\Lambda \subset \mathbb{R}^n$, let $V(\Lambda; p)$ be the open Voronoi domain of a point $p \in \Lambda$. The *neighbor set* $N(\Lambda; p)$ consists of all points that appear among the first $n + 1$ nearest neighbors within $\Lambda - p$ for some interior point $q \in V(\Lambda; p)$ whose first neighbor is p . Let $p = (0, 0)$. If $\Lambda = \mathbb{Z}^2$, then $N(\Lambda; p) = \{(\pm 1, 0), (0, \pm 1)\}$. For Λ generated by $(2, 0), (0, 1)$, the neighbor set $N(\Lambda; p)$ also includes the 3rd neighbors $(0, \pm 2)$ of the points $q = (0, \pm 0.4) \in V(\Lambda; p)$.

For any point $q \in V(\Lambda; p)$, consider all n -tuples (p_1, \dots, p_n) of points $p_i \in N(\Lambda; p)$ such that the vectors $p_i - p$, $i = 1, \dots, n$, form a linear basis of \mathbb{R}^n . Order the points of (p_1, \dots, p_n) by their distances to q (uniquely if all distances are distinct). Choose the lexicographically smallest list of *basis distances* $d_1 \leq \dots \leq d_n$ from q over all n -tuples (p_1, \dots, p_n) above.

► **Definition 8** (a distance-generic periodic point set). A periodic point set $S = \Lambda + M \subset \mathbb{R}^n$ with a primitive unit cell U is called *distance-generic* if the following conditions hold.

- (8a) For any $p \in M$ and points $q, r \in S \cap V(\Lambda; p)$, the vectors $q - p, r - p$ are not orthogonal.
- (8b) For any vectors \vec{u}, \vec{v} between two pairs of points in S , if $|\vec{u}| = l|\vec{v}| \leq 2\text{diam}[U]$ for $l = 1, 2$, then $\vec{u} = \pm l\vec{v}$ and $\vec{v} \in \Lambda$, hence the cell U has different edge-lengths and no right angles.
- (8c) For any points $p_0 \in M$ and $q \in V(\Lambda; p_0)$, let d_0 be the distance from q to its closest neighbor p_0 within $p_0 + \Lambda$. Take any p_1, \dots, p_n in the neighbor set $N(\Lambda; p_0)$ with distances $d_1 \leq \dots \leq d_n$ to q . Then the $n + 1$ spheres $C(p_i; d_i)$ with the centers p_i and radii d_i , $i = 0, \dots, n$, can meet at a single point in $V(\Lambda; p_0)$ only if $d_1 \leq \dots \leq d_n$ are the basis distances of q , the vectors $p_i - p_0$, $i = 1, \dots, n$ form a linear basis of \mathbb{R}^n , and only for at most two tuples $p_1, \dots, p_n \in N(\Lambda; p_0)$ that are symmetric to each other with respect to p_0 . ■

Condition (8b) means that all inter-point distances are distinct apart from necessary exceptions due to periodicity. Since any periodic set $S = \Lambda + M \subset \mathbb{R}^n$ is invariant under translations along vectors of its lattices Λ , condition (8b) can be checked only for vectors from points in a unit cell U to points in the extended motif $S \cap (3U)$ for $3U = \{3\vec{v} \mid \vec{v} \in U\}$.

Almost all $n + 1$ spheres in \mathbb{R}^n have no common points, hence condition (8c) forbids very singular situations, which can be practically checked since the neighbor set $N(\Lambda; p_0)$ is finite for any lattice Λ and its point p_0 . All conditions of Definition 8 can be written as algebraic equations via coordinates of motif points and basis vectors of a unit cell. Hence any periodic point set can be made distance-generic by almost any small perturbation of points.

► **Theorem 9** (generic completeness of PDD). *Let $S = \Lambda + M \subset \mathbb{R}^n$ be a distance-generic periodic set with m points in a unit cell U . Choose k so that the smallest distance value in the last k -th column of $\text{PDD}(S; k)$ is at least $2\text{diam}[U]$. The set $S \subset \mathbb{R}^2$ can be uniquely reconstructed up to isometry from $\text{PDD}(S; k)$ and m . For $n = 3$, the set $S \subset \mathbb{R}^3$ can be uniquely reconstructed up to isometry from $\text{PDD}(S; k)$, m and the six conorms p_{ij} of Λ . ■*

297 *Short proof.* Using rational weights of rows in $\text{PDD}(S; k)$, we expand this matrix so that all
 298 m rows have equal weights, hence correspond to m points in a motif of S , which is built
 299 below. For any lattice $\Lambda \subset \mathbb{R}^2$ with an obtuse superbase $\vec{v}_0, \vec{v}_1, \vec{v}_2$, condition (8b) helps
 300 recognize $|\vec{v}_0|, |\vec{v}_1|, |\vec{v}_2|$ as three shortest distances (appearing with their doubles) in every
 301 row of $\text{PDD}(S; k)$, see [12, Theorem 7] and reconstruct Λ . Any $\Lambda \subset \mathbb{R}^3$ is reconstructed from
 302 its six conorms p_{ij} , see [12, section 8]. After we built Λ containing (say) $p_0 = 0$, we remove
 303 from each row of $\text{PDD}(S; k)$ all distances from any point p to its lattice translates $p + \Lambda$.

304 Any other point $q \in S$ in the open Voronoi domain $V(\Lambda; 0)$ has its lexicographically
 305 smallest list of basis distances $d_1 < \dots < d_n$ from q to $p_1, \dots, p_n \in N(\Lambda; 0)$. The basis
 306 distances appear once in both rows of $p_0 = 0$ and q in $\text{PDD}(S; k)$ after the shortest distance
 307 $d_0 = |q - p_0| = |q|$. Trying all n -distance subsequences $d'_1 < \dots < d'_n$ appearing in both rows
 308 of $p_0 = 0$ and q , and also trying all n -tuples of points $p_1, \dots, p_n \in N(\Lambda; 0)$ that form a linear
 309 basis of \mathbb{R}^n , we check if the $n + 1$ spheres $S(p_i; d'_i)$ meet at a single point in $V(\Lambda; 0)$.

310 By condition (8c) a single-point intersection, which will be our point q , is possible only for
 311 the basis distances $d_1 < \dots < d_n$ of q and only for two n -tuples $p_1, \dots, p_n \in N(\Lambda; 0)$ related
 312 by the symmetry with respect to 0. We can choose one of two possible positions of q since
 313 this symmetry is an isometry preserving Λ . For any further point $p \neq 0, q$, there is no choice
 314 due to the available distance $|p - q|$ and condition (8a), see more details in Appendix B. \square

315 **6 Polynomial time algorithms and a discussion of $\text{PDD}^{\{h\}}$ significance**

316 This section presents the main algorithmic result for $\text{PDD}^{\{h\}}$, which has allowed us to
 317 thoroughly check the world's largest database of hundreds of thousands of real structures.

318 **► Theorem 10** ($\text{PDD}^{\{h\}}$ complexity). *Let a periodic set $S \subset \mathbb{R}^n$ have m points in a unit cell*
 319 *U . Then $\text{PDD}^{\{h\}}(S; k)$ is computed in time $O(h^2 km^h (5\nu)^n V_n \log(hm) \log^2 k)$, where V_n is*
 320 *the unit ball volume in \mathbb{R}^n , d and $\nu = \frac{d}{\sqrt[n]{\text{Vol}[U]}}$ are the diameter and skewness of U . \blacksquare*

321 *Short proof.* For any point $p \in S$, let $d_k(S; p)$ be the distance to its k -th nearest neighbor in
 322 S . Then $d_k(S; p) \leq c(S) \sqrt[k]{k} + d$, where d is the diameter of U of S and $c(S) = \sqrt[n]{\frac{\text{Vol}[U]}{mV_n}}$,
 323 V_n is the volume of the unit ball in \mathbb{R}^n . We find all k nearest neighbors of motif points
 324 $p \in M = S \cap U$ by adding ‘spherical’ layers around the initial cell U . The total number of
 325 points from S in this extension is at most $\mu = \left(\sqrt[k]{k} + \frac{2.5d}{c(S)} \right)^n = O(2^n (k + m(2.5\nu)^n V_n))$.
 326 After computing a cover tree [7] on μ points in time $O(\mu \log \mu)$, the time for $\text{PDD}(S; k)$ for
 327 $h = 1$ is $O(\mu \log \mu + mk \log^2 k) = O(km(5\nu)^n V_n \log m \log^2 k)$, see details in appendix B. \square

328 A detailed pseudo-code is in appendix A. Most real structures have a small skewness
 329 ν . If ν is fixed, then $(5\nu)^n V_n \rightarrow 0$ as $n \rightarrow +\infty$ by Stirling's approximation. For practical
 330 dimensions $n = 2, 3$, the key input sizes are the number k of neighbors and the number m of
 331 motif points. Hence the near linear and quadratic dependencies on k, m are most crucial.

332 We conjecture that any finite or periodic sets $S \subset \mathbb{R}^n$ is uniquely determined up to
 333 isometry by $\text{PDD}^{\{h\}}(S; k)$ for $h = n - 1$ and a sufficiently large k depending on S . Theorem 9
 334 has proved this for $h = 1$ and any $n = 2, 3$ in general position. Actual data of all real and
 335 simulated structures contains measurement noise and floating point errors, which makes
 336 many structures generic in practice. Moreover, $\text{PDD}^{\{h\}}$ can distinguish non-generic sets, see
 337 Examples 16, 17, 18 in appendix C for all known counter-examples to past invariants.

338 We computed $\text{AMD}(S; 100)$ obtained from $\text{PDD}(S; 100)$ by column averaging for all 229K
 339 known molecular organic crystals in the Cambridge Structural Database. The L_∞ -distance
 340 between the vectors $\text{AMD}(S; 100)$ was less than 0.01 for 2483 pairs, which turned out to be
 341 identical or near duplicates by the traditional and much slower RMSD comparison [11].

342 Much more importantly, since all real structures were distinguished above, the map
 343 from real crystals to isometry classes of periodic point sets is injective. Hence the space of
 344 all crystals is continuously parameterized by $\text{PDD}^{\{h\}}$, a sought-after DNA-type code for a
 345 guided discovery of new materials. Such a continuous map will substantially extend a simpler
 346 discrete parameterization of all chemical elements known as Mendeleev’s periodic table.

347 **A Appendix A: pseudocode of the polynomial time $\text{PDD}^{\{h\}}$ algorithm**

348 This appendix describes the algorithm from Theorem 10 for the higher order Pointwise
 349 Distance Distribution $\text{PDD}^{\{h\}}$ in greater detail.

350 The algorithm takes any periodic point set $S \subset \mathbb{R}^n$ in the form of a unit cell U and a
 351 motif $M \subset S$ in the basis of U . A unit cell can be given by a linear basis of n vectors. Then
 352 every point $p \in M$ is given by coordinates in this basis. The implemented code in Python
 353 takes any Crystallographic Information File of a 3D crystal containing the above parameters.
 354 The code also works for periodic sets in 1D and 2D, extensions to $n > 3$ are straightforward.

355 In addition to a periodic point set S , the only other part of the input are a number k
 356 of neighbors and an order h of Pointwise Distance Distributions. These k and h are not
 357 usual parameters that affect an output, but can be considered as orders of approximation,
 358 i.e. increasing k includes extra information between more distant neighbors. All results for
 359 lower values of k remain unchanged in the output for any larger k . Here are the key stages

360 **Neighboring stage 1.** Find the first $k + h - 1$ nearest neighbors to each motif point within
 361 the given periodic set S by using fast k-d trees.

362 **Distancing stage 2.** Compute ordered lists of distances from points in every subset $A \subset M$
 363 of h points within the motif of m points.

364 **Ordering stage 3.** Lexicographically order rows, collapse identical rows, assign weights to
 365 rows for the final $\text{PDD}^{\{h\}}(S; k)$.

366 In the output the first order $\text{PDD}(S; k)$ is a matrix with at most m rows (if all different)
 367 and exactly $k + 1$ columns, where m is the number of points in a motif M (or in a unit cell
 368 U). The first column of $\text{PDD}(S; k)$ includes weights of rows (default values $1/m$ if all rows
 369 are different).

370 The second order $\text{PDD}^{\{2\}}(S; k)$ is also a matrix with $k + 2$ columns, which are more
 371 diverse. The extra 2nd column contains distances between unordered pairs of points. The k
 372 columns from 3 to $k + 2$ contain pairs of distances. The lexicographic ordering of rows in
 373 $\text{PDD}^{\{2\}}$ compares distances in the 2nd column, then pairs of ordered distances one by one.

374 The higher order distributions $\text{PDD}^{\{h\}}(S; k)$ are even more diverse. The 2nd column
 375 contains the matrices $D(A; h - 1)$ from Definition 3 for finite unordered subsets $A \subset M$ of h
 376 points in a motif of S . In the case $h = 2$, the matrix $D(A; h - 1)$ consists of a single distance
 377 between two points. For $h > 2$ and each point $p \in A$, we order its distances to all other $h - 1$
 378 points in A . Then we lexicographically order the resulting h lists of distances to form the
 379 $h \times (h - 1)$ matrix $D(A; h - 1)$. Then all elements of the 2nd column in $\text{PDD}^{\{h\}}(S; k)$ have
 380 the same size $h \times (h - 1)$, hence can be lexicographically compared when ordering rows in
 381 $\text{PDD}^{\{h\}}(S; k)$. Here is the Python interface of the $\text{PDD}^{\{h\}}$ code.

```
382     PDD(motif, cell, k, h=1)
```

383 Returns $\text{PDD}^{\{h\}}(S; k)$ for a periodic set $S \subset \mathbb{R}^n$ represented by `motif` and `cell`.

384 Input:

- 385 ■ `motif`: `np.ndarray` shape (m, n) . Cartesian coordinates of motif points in the unit cell.
- 386 ■ `cell`: `np.ndarray` shape (n, n) . Square matrix representing the unit cell in Cartesian form. (`ase.geometry.cellpar_to_cell` converts $[a, b, c, \alpha, \beta, \gamma]$ to Cartesian form.)
- 387 ■ `k`: `int` > 0 . Number of columns to return in $\text{PDD}^{\{h\}}(S; k)$.
- 388 ■ `h`: `int` > 0 , default 1. Order of the $\text{PDD}^{\{h\}}$ invariant.

390 Output:

- 391 ■ `np.ndarray` (structured array) representing $\text{PDD}^{\{h\}}(S; k)$. The array is a vector length t , where $t \leq C_h^m$ depends on the number of identical rows of distances that are collapsed.
- 392 The `dtype` (layout) of each row depends on h :
- 393 ■ $h = 1$: (float, array)
- 394 ■ $h = 2$: (float, float, array)
- 395 ■ $h > 2$: (float, array, array)
- 396 If the result is assigned to the name `arr`, elements can be accessed as follows:
- 397 ■ `arr['weight']` (first column) the vector of weights, shape $(t,)$
- 398 ■ `arr['dist']` (second column) a vector of floats when $h = 2$, a vector of arrays if $h > 2$
- 399 and is not present when $h = 1$
- 400 ■ `arr['pdd']` (all other columns) the main distance distribution matrix, of shape (t, k, h)
- 401 (last dimension removed if $h = 1$).
- 402

403 A.1 Stage 1: Nearest neighbors to motif points

404 The outline of this step is straightforward, after describing the core objects in use:

- 405 ■ A generator object `g`, which creates points from the periodic set S for use in distance calculations,
- 406 ■ `KDTree`s (canonically k is the dimension here, in our case it's denoted n), data structures designed for fast nearest-neighbour lookup in n -dimensional space.

409 Once `g` is constructed, `next(g)` is called to get new points from S . The first call returns all points in the 'main' unit cell described by `cell` (i.e. the motif), and successive calls return points from unit cells further from the origin in a spherical fashion.

412 A `KDTree` is constructed with a point set T , then queried with another Q , returning a matrix with distances from all points in Q to their nearest neighbors (up to some given number, q below) in T , as well as the indices of these neighbors in T .

415 The following pseudocode gets the first q neighbours:

```
416     cloud = [] # contains points from S
417     g = point_generator(motif, cell)
418
419     ## at least q points will be needed
420     while len(cloud) < q:
421         points = next(g)
422         cloud.extend(points)
423
424     ## first distance query
425     tree = KDTree(cloud)
```

```

426     D_, inds = tree.query(motif, q)
427     D = zeros_like(D_)    # copy of D_, but all zeros
428
429     ## repeat until distances don't change,
430     ## then all nearest neighbors are found
431     while not D == D_:
432         D = D_
433         cloud.extend(next(g))
434         tree = KDTree(cloud)
435         D_, inds = tree.query(motif, q)
436

```

437 In implementation, `cloud`, `D_` and `inds` are all returned to be used in the next step.

438 A.2 Stage 2: main distance constructions

439 This stage is skipped for $h = 1$, because all necessary distances were already found in stage 1.
440 From step 1, we have (1) a set `cloud` of points from S , (2) a matrix `D_` of nearest neighbor
441 distances for each `motif` point (up to $k + h - 1$ neighbors), and (3) a matrix `inds` of the
442 indexes of these neighbors in `cloud`.

443 We construct the PDD (and dists column) row-by-row, element-by-element. For a given
444 row, `points` contains (the indexes of) points in the corresponding unordered set. We initialise
445 a list `pointers` of h zeros, which are indices into `D_` and `inds`. They start pointing at the
446 first elements, i.e. the nearest neighbors to `points`. We also create a set `done` containing
447 points to be ignored as neighbors, at first just containing `points`.

448 Before adding an element to a row, we increment all `pointers` until they don't point to
449 an element of `done`. Now, `pointers` point to the next h candidates for nearest neighbor to
450 the unordered set. We find which is closest, compute distances from that point to `points`
451 and sort, appending the new element to the row. We then also find the next element in the
452 dist column, which is different for $h = 2$ and $h > 2$.

```

453 pdd = []
454 dist = []
455
456 for points in combinations(range(m), 2):
457
458     done = set(points)
459     pointers = [0] * h
460
461     ## construct row
462     row = []
463     for _ in range(k):
464
465         ## pointer update
466         for i in range(h):
467             while inds[points[i]][pointers[i]]
468                 in done:
469                 pointers[i] += 1
470

```

```

471     # index of point with the closest neighbor
472     p = argmin([D_[points[i]][pointers[i]]
473                for i in range(h)])
474
475     # index of said neighbour in cloud
476     point = inds[points[p]][pointers[p]]
477
478     # add to element to row
479     row.append(
480         sorted(
481             euclidean(motif[points[i]],
482                      cloud[point])
483             for i in range(h)
484         )
485     )
486
487     # update done and pointer
488     done.add(point)
489     pointers[p] += 1
490
491     pdd.append(row)
492
493     ## add to dist
494     if h == 2:
495         d = euclidean(motif[points[0]],
496                      motif[points[1]])
497     else:
498         d = finite_PDD(motif[points])
499     dist.append(d)

```

500 Final stage 3 requires only standard operations of lexicographic ordering.

```

501 ## example: PDD for the lowest energy T2- $\epsilon$  crystal from \cite{pulido2017functional}
502
503 >>> cell = [[12.607  0.    0.    ]
504             [-6.303  10.91  0.    ]
505             [ 0.    0.    7.493]]
506 >>> motif = [[ 11.221  1.564  1.873]
507             [ 9.750  0.120  2.972]
508             ...
509             [-3.446  10.798  4.520]
510             [-3.625  10.586  3.685]]
511
512 >>> PDD(motif, cell, k=20, h=1)
513
514 # output: weights in first column
515 [[0.011 0.880 1.369 ... 3.367 3.372 3.568]
516  [0.011 0.880 1.369 ... 3.367 3.372 3.568]
517  ...

```

```

518     [0.011 1.390 1.394 ... 3.563 3.765 3.813]
519     [0.011 1.390 1.394 ... 3.563 3.765 3.813]]
520
521 >>> PDD(motif, cell, k=20, h=2)
522
523 # output: columns separated by keys in a dict.
524 {
525     'weights':
526         [2.3e-4, 2.3e-4, ..., 2.3e-4, 2.3e-4],
527     'dists':
528         [0.88, 0.88, ..., 18.3, 18.5],
529     'matrix':
530         [[ [1.37,2.01], [1.39,2.03], ..., [3.56,4.33] ],
531          [ [1.37,2.01], [1.39,2.03], ..., [3.56,4.33] ],
532           ...
533          [ [1.25,17.9], [1.25,17.9], ..., [3.11,21.1] ],
534          [ [0.88,18.9], [0.88,18.9], ..., [2.82,18.3] ] ]
535 }
```

536 **B** Appendix B: detailed proofs of Theorems 5, 7, 9, 10

537 **Full proof of Theorem 5.** For periodic sets, first we show that $D(S; k)$ from Definition 3,
538 hence $\text{PDD}^{\{h\}}(S)$, is independent of a primitive unit cell. Let U, U' be primitive cells of a
539 periodic set $S \subset \mathbb{R}^n$ with a lattice Λ . Any point $q \in S \cap U'$ can be translated by some $\vec{v} \in \Lambda$
540 to a point $p \in S \cap U$ and vice versa. These translations establish a bijection between the
541 motifs $S \cap U \leftrightarrow S \cap U'$ and preserve distances. So $\text{PDD}^{\{h\}}(S; k)$ is the same for both U, U' .

542 Now we prove that $\text{PDD}^{\{h\}}(S; k)$ is preserved by any isometry $f : S \rightarrow Q$. Any primitive
543 cell U of S is bijectively mapped by f to the unit cell $f(U)$ of Q , which should be also
544 primitive. Indeed, if Q is preserved by a translation along a vector \vec{v} that doesn't have all
545 integer coefficients in the basis of $f(U)$, then $S = f^{-1}(Q)$ is preserved by the translation
546 along $f^{-1}(\vec{v})$, which also doesn't have all integer coefficients in the basis of U , i.e. U was
547 non-primitive. Since both primitive cells U and $f(U)$ contain the same number of points
548 from S and $Q = f(S)$, the isometry f gives a bijection between the motifs of S, Q .

549 For any finite or periodic sets S, Q , since f preserves distances, every list of ordered
550 distances from $p_i \in S \cap U$ to its first k nearest neighbors in S , coincides with the list of the
551 ordered distances from $f(p_i)$ to its first k neighbors in Q . These coincidences of distance
552 lists give $\text{PDD}^{\{h\}}(S; k) = \text{PDD}^{\{h\}}(Q; k)$ after collapsing identical rows. ◀

553 Lemmas 11, 12, 13 are needed to prove Theorem 7.

554 ▶ **Lemma 11** (perturbed distances). For some $\varepsilon > 0$, let $g : S \rightarrow Q$ be a bijection between
555 finite or periodic sets such that $|a - g(a)| \leq \varepsilon$ for all $a \in S$. Then, for any $i \geq 1$, let $a_i \in S$
556 and $b_i \in Q$ be the i -th nearest neighbors of points $a \in S$ and $b = g(a) \in Q$, respectively.
557 Then the Euclidean distances from the points a, b to their i -th neighbors a_i, b_i are 2ε -close
558 to each other, i.e. $||a - a_i| - |b - b_i|| \leq 2\varepsilon$. ■

559 **Proof.** Shifting the point $g(a)$ back to a , assume that $a = g(a)$ is fixed and all other points
560 change their positions by at most 2ε . Assume by contradiction that the distance from a to
561 its new i -th neighbor b_i is less than $|a - a_i| - 2\varepsilon$.

562 Then all first new i neighbors b_1, \dots, b_i of a within Q belong to the open ball with the
 563 center a and the radius $|a - a_i| - 2\varepsilon$. Since the bijection g shifted every b_1, \dots, b_i by at most
 564 2ε , their preimages $g^{-1}(b_1), \dots, g^{-1}(b_i)$ belong to the open ball with the center a and the
 565 radius $|a - a_i|$.

566 Then the i -th neighbor of a within S is among these i preimages, i.e. the distance from a
 567 to its i -th nearest neighbor should be strictly less than the assumed value $|a - a_i|$.

568 Similarly get a contradiction assuming that the distance from a to its new i -th neighbor
 569 b_i is more than $|a - a_i| + 2\varepsilon$. ◀

570 ▶ **Lemma 12** (perturbed distance vectors). For $\varepsilon > 0$, let $g : S \rightarrow Q$ be a bijection between
 571 finite or periodic sets so that $|a - g(a)| \leq \varepsilon$ for all $a \in S$. Then, for $k \geq 1$, the bijection
 572 g changes the vector $\vec{R}_a(S) = (|a - a_1|, \dots, |a - a_k|)$ of the first k minimum distances
 573 from any point $a \in S$ to its k nearest neighbors $a_1, \dots, a_k \in S$ by at most 2ε in the
 574 L_∞ -distance. So if $b_1, \dots, b_k \in Q$ are the k nearest neighbors of $b = g(a)$ within Q and
 575 $\vec{R}_b(Q) = (|b - b_1|, \dots, |b - b_k|)$ is the vector of the first k minimum distances from $b = g(a)$,
 576 then the L_∞ -distance $|\vec{R}_a(S) - \vec{R}_b(Q)|_\infty \leq 2\varepsilon$. ■

577 **Proof.** By Lemma 11 every coordinate of the vector $\vec{R}_a(S)$ changes by at most 2ε . Hence
 578 the L_∞ -distance from $\vec{R}_a(S)$ to the perturbed vector $\vec{R}_b(Q)$ is at most 2ε . ◀

579 ▶ **Lemma 13** (common lattice). Let periodic point sets $S, Q \subset \mathbb{R}^n$ have a bottleneck distance
 580 $d_B(S, Q) < r(Q)$, where $r(Q)$ is the packing radius. Then S, Q have a common lattice Λ
 581 with a unit cell U such that $S = \Lambda + (U \cap S)$, $Q = \Lambda + (U \cap Q)$. ■

582 **Proof.** Let $S = \Lambda(S) + (U(S) \cap S)$ and $Q = \Lambda(Q) + (U(Q) \cap Q)$, where $U(S), U(Q)$ are
 583 initial unit cells of S, Q and the lattices $\Lambda(S), \Lambda(Q)$ of S, Q contain the origin.

584 By shifting all points of S, Q (but not their lattices), we guarantee that S contains the
 585 origin 0 of \mathbb{R}^n . Assume by contradiction that the given periodic point sets S, Q have no
 586 common lattice. Then there is a vector $\vec{p} \in \Lambda(S)$ whose all integer multiples $k\vec{p} \notin \Lambda(Q)$ for
 587 $k \in \mathbb{Z} - 0$. Any such multiple $k\vec{p}$ can be translated by a vector $\vec{v}(k) \in \Lambda(Q)$ to the initial
 588 unit cell $U(Q)$ so that $\vec{q}(k) = k\vec{p} - \vec{v}(k) \in U(Q)$.

589 Since $U(Q)$ contains infinitely many points $\vec{q}(k)$, one can find a pair $\vec{q}(i), \vec{q}(j)$ at a
 590 distance less than $\delta = r(Q) - d_B(S, Q) > 0$. The formula $\vec{q}(k) \equiv k\vec{p} \pmod{\Lambda(Q)}$ implies that
 591 $\vec{q}(i + k(j - i)) \equiv (i + k(j - i))\vec{p} \pmod{\Lambda(Q)} \equiv \vec{q}(i) + k(\vec{q}(j) - \vec{q}(i)) \pmod{\Lambda(Q)}$. If the point
 592 $\vec{q}(i) + k(\vec{q}(j) - \vec{q}(i))$ belongs to $U(Q)$, we get the equality $\vec{q}(i + k(j - i)) = \vec{q}(i) + k(\vec{q}(j) - \vec{q}(i))$.
 593 All these points over $k \in \mathbb{Z}$ lie on a straight line within $U(Q)$ and have the distance
 594 $|\vec{q}(j) - \vec{q}(i)| < \delta$ between successive points.

595 The closed balls with radius $d_B(S, Q)$ and centers at points in Q are at least 2δ away
 596 from each other. Then one of the points $\vec{q}(i + k(j - i))$ is more than $d_B(S, Q)$ away from Q .
 597 Hence the point $(i + k(j - i))\vec{p} \in S$ also has a distance more than $d_B(S, Q)$ from any point
 598 of Q , which contradicts the definition of the bottleneck distance. ◀

599 **Full proof of Theorem 7 for $h = 1$.** Recall that the bottleneck distance is defined as
 600 $d_B(S, Q) = \inf_{g: S \rightarrow Q} \sup_{a \in S} |a - g(a)|$ between point sets S, Q . Then for any $\delta > 0$ there is a
 601 bijection $g : S \rightarrow Q$ such that $\sup_{a \in S} |a - g(a)| \leq d_B(S, Q) + \delta$.

602 If the given sets S, Q are finite, one can set $\delta = 0$. Indeed, there are only finitely many
 603 bijections $S \rightarrow Q$, hence the infimum in the definition above is achieved for one of them.

604 By Lemma 13 if the sets S, Q are periodic, they have a common lattice Λ . Any primitive
 605 cell U of Λ is a unit cell of S, Q , i.e. $S = \Lambda + (S \cap U)$ and $Q = \Lambda + (Q \cap U)$. Since the
 606 bottleneck distance $\varepsilon = d_B(S, Q) < \frac{r(S)}{4}$, we can define a bijection g from every point $a \in S$
 607 to a closest point $g(a) \in Q$. If U is a non-primitive unit cell of S , the distance matrix $D(S; k)$
 608 can be constructed as in Definition 3, but each row will be repeated $n(S)$ times, where $n(S)$
 609 is $\text{Vol}[U]$ divided by the volume of a primitive unit cell of S . So we can assume that S, Q
 610 share a unit cell U and have in U the same number $m(S) = m(Q)$, say both are equal to m .

611 For any $k \geq 1$, we first define the simple 1-1 flow from the rows of $D(S; k)$ to the rows of
 612 $D(Q; k)$ by setting $f_{ii} = \frac{1}{m}$ and $f_{ij} = 0$ for $i \neq j$, where $i, j = 1, \dots, m$.

613 Recall that Definition 3 collapses all rows of $D(S; k)$ that are identical to each other
 614 to a single row, similar for $D(Q; k)$. By summing up weights of collapsed rows, the above
 615 flow induces a flow from all distance vectors in $\text{PDD}(S; k)$, e.g. $R_i(S)$ in the i -th row of
 616 $\text{PDD}(S; k)$, to all distance vectors in $\text{PDD}(Q; k)$.

617 Then $\text{EMD}(\text{PDD}(S; k), \text{PDD}(Q; k)) \leq \frac{1}{m} \sum_{i=1}^m |\vec{R}_i(S) - \vec{R}_i(Q)|_\infty$, because EMD minimizes
 618 the cost over all flows in Definition 6. Since each $|\vec{R}_i(S) - \vec{R}_i(Q)| \leq 2(d_B(S, Q) + \delta)$
 619 by Lemma 12, we conclude that $\text{EMD}(\text{PDD}(S; k), \text{PDD}(Q; k)) \leq \frac{1}{m} \sum_{i=1}^m 2(d_B(S, Q) + \delta) =$
 620 $2(d_B(S, Q) + \delta)$. Since the last inequality holds for any small $\delta > 0$, we get the required
 621 continuity $\text{EMD}(\text{PDD}(S; k), \text{PDD}(Q; k)) \leq 2d_B(S, Q)$. ◀

622 **Full proof of Theorem 7 for $h > 1$.** The proof follows the easier case $h = 1$. The rows of
 623 $\text{PDD}^{\{h\}}(S; k)$ are indexed by $m_h(S) = \frac{m(S)!}{h!(m(S) - h)!}$ unordered subsets $A \subset S$ of h points.
 624 Here $m(S)$ is the number of points in a motif of S .

625 The first component of a row R_A in $\text{PDD}^{\{h\}}(S; k)$ is $D(A)$ from Definition 4. The distance
 626 between these matrices for subsets $A \subset S$ and $g(A) \subset Q$ is computed as $d(A, g(A)) =$
 627 $|D(A) - D(g(A))|_\infty \leq 2d_B(S, Q)$. Indeed, we turn $D(A)$ into a vector by concatenating all
 628 rows. The corresponding rows in $D(A), D(g(A))$ are close by Lemma 12.

The L_∞ -distance between the remaining lists of h ordered distances to h points in the
 subsets A and $g(A)$ has the same upper bound $2d_B(S, Q)$ by Lemma 12. Hence the upper
 bound $2d_B(S, Q)$ emerges unchanged through the estimate

$$\text{EMD}(\text{PDD}^{\{h\}}(S; k), \text{PDD}^{\{h\}}(Q; k)) \leq$$

$$\frac{1}{m_h(S)} \sum_{|A|=h} \max \left\{ d(A, g(A)), |\vec{R}_A(S) - \vec{R}_{g(A)}(Q)|_\infty \right\}$$

629 $\leq 2d_B(S, Q)$, where $m_h(S)$ is the number of unordered subsets of h points chosen from
 630 $m(S) = m(Q)$ points. ◀

631 **Full proof of Theorem 9.** Assuming that the first order $\text{PDD}(S; k)$ is realizable by a periodic
 632 point set $S = \Lambda + M$, we explain below how to reconstruct a lattice Λ containing (say) the
 633 origin (uniquely up to isometry), then a motif of S in the Voronoi domain $V(\Lambda; 0)$, uniquely
 634 up a central symmetry preserving Λ .

635 Let l be the lowest common multiple of all denominators in rational weights of the rows
 636 in the given matrix $\text{PDD}(S; k)$. Then every row of weight j/l can be replaced by j identical

637 rows of weight $1/l$. The number m of points in a given unit cell U can be considered as an
 638 isometry invariant, because any isometry maps a unit cell to another unit cell with the same
 639 number of points. If $l < m$, for example, if all m points $p \in M$ have isometrically equivalent
 640 neighborhoods $(S, p) = \{q - p \mid q \in S\}$, so $l = 1$, then we know that every row should
 641 be multiplied m/l times. Now we forget about these equal weights and will reconstruct a
 642 periodic point set S with a motif M of m points.

643 Condition (8b) for any point $p \in M$, allows us to recognize *lattice distances* from p to
 644 its lattice translates $p + \Lambda$ within the row of $\text{PDD}(S; k)$ representing p . Indeed, only such a
 645 lattice distance d appears in the row together with $2d$ (and possibly with higher multiples)
 646 by condition (8b). Moreover, any lattice distance d and its multiple is repeated twice in
 647 every row, because any lattice is centrally symmetric.

648 Every row contains several such distinct distances d between p and $p + \vec{v}$ for non-parallel
 649 vectors $\vec{v} \in \Lambda$. In dimension $n = 2$, we consider only the first three such shortest distances
 650 $d_0 < d_1 < d_2$ repeated exactly twice in every row. If we start building a lattice $\Lambda \subset \mathbb{R}^2$
 651 from the origin 0 , then $d_0 < d_1 < d_2$ are the distances from 0 to three symmetric pairs of
 652 Voronoi neighbors of 0 within Λ . By [12, Theorem 7], these distances equal the lengths of
 653 vectors $\vec{v}_0, \vec{v}_1, \vec{v}_2 \in \Lambda$ that form an obtuse superbase of Λ meaning that $\vec{v}_0 + \vec{v}_1 + \vec{v}_2 = 0$ and
 654 $p_{ij} = -\vec{v}_i \cdot \vec{v}_j \geq 0$ for distinct $i, j \in \{0, 1, 2\}$. Using d_0, d_1, d_2 as edge-lengths, we can build a
 655 triangle (unique up to isometry) on the vectors $-\vec{v}_0 = \vec{v}_1 + \vec{v}_2, \vec{v}_1, -\vec{v}_2$ and get a unit cell U
 656 of Λ . Since $d_0 < d_1 < d_2 \leq \text{diam}[U]$, the above distances and their doubles are included into
 657 every row of $\text{PDD}(S; k)$, hence can be recognized above.

658 The above argument is insufficient for $n \geq 3$. However, any lattice $\Lambda \subset \mathbb{R}^3$ has an obtuse
 659 superbase $\vec{v}_0, \vec{v}_1, \vec{v}_2, \vec{v}_3$ such that $\vec{v}_0 + \vec{v}_1 + \vec{v}_2 + \vec{v}_3 = 0$ and $p_{ij} = -\vec{v}_i \cdot \vec{v}_j \geq 0$ for distinct
 660 $i, j \in \{0, 1, 2, 3\}$. These six conorms p_{ij} are continuous isometry invariants that suffice to
 661 reconstruct Λ up to isometry [12, section 8]. For $n = 2$, a lattice $\Lambda \subset \mathbb{R}^2$ can be similarly
 662 reconstructed from its three conorms, which are extractable from $\text{PDD}(S; k)$ as above.

663 Without loss of generality one can assume that a reconstructed lattice Λ contains the
 664 origin $p_0 = 0$ represented by the first row of $\text{PDD}(S; k)$. If this matrix has $m \geq 2$ rows, we
 665 will reconstruct all other $m - 1$ points of S within the open Voronoi domain $V(\Lambda; 0)$. No
 666 points of S can be on the boundary of $V(\Lambda; 0)$ due to condition (8b) on distinct distances.

667 First we remove from each row of $\text{PDD}(S; k)$ all lattice distances so that every remaining
 668 distance is from a point p to a point $q \notin p + \Lambda$. Any other point $q \in S$ in the open Voronoi
 669 domain $V(\Lambda; 0)$ has its lexicographically smallest list of basis distances $d_1 < \dots < d_n$ from q
 670 to its closest lattice points $p_1, \dots, p_n \in N(\Lambda; 0) \subset \Lambda$ subject to the condition that the vectors
 671 $p_i - p_0 = p_i$ form a basis of \mathbb{R}^n . The basis distances are distinct by (8b) and appear once in
 672 both rows of $p_0 = 0$ and q in $\text{PDD}(S; k)$ after the shortest distance $d_0 = |q - p_0| = |q|$ from
 673 q to Λ . Indeed, the maximum $(n + 1)$ -st distance (for $n = 2$ or $n = 3$) from q to Λ cannot be
 674 longer than a maximum distance to a corner of a unit cell U so $\text{diam}[U]$ is an upper bound.
 675 Hence all basis distances of any point $q \in S \cap V(\Lambda; 0)$ are contained in $\text{PDD}(S; k)$.

676 Though the basis distances of q may not be the n smallest values appearing after $d_0 = |q|$
 677 in the first and second rows of 0 and q , we will try all n -distance subsequences $d'_1 < \dots < d'_n$
 678 shared by both rows. Similarly, we cannot be sure that n closest neighbors of q in Λ form
 679 a basis of \mathbb{R}^n , hence we will try all n -tuples of points $p_1, \dots, p_n \in N(\Lambda; 0)$ that form a
 680 linear basis of \mathbb{R}^n . The condition of a linear basis is needed to guarantee that $n + 1$ affinely
 681 independent points $p_0 = 0, p_1, \dots, p_n$ uniquely identify a point q by their distances to q . For

all finitely many choices above, we check if the $n + 1$ spheres $S(p_i; d'_i)$, which are 1D circles (for $n = 2$) or 2D spheres (for $n = 3$), meet at a single point in $V(\Lambda; 0)$, which will be q .

Condition (8c) guarantees that these $n + 1$ spheres can intersect at a single point in the open Voronoi domain $V(\Lambda; 0)$ only if the three conditions below hold. Firstly, the vectors of the points p_1, \dots, p_n should form a linear basis of \mathbb{R}^n . Secondly, the distances $d'_1 < \dots < d'_n$ equal the basis distances $d_1 < \dots < d_n$ of q meaning that this list is the lexicographically smallest over all tuples $\{p_1, \dots, p_n\} \subset N(\Lambda; 0)$ that form a linear basis. Thirdly, the single-point intersection happens only for two subsets $\{p_1, \dots, p_n\} \subset N(\Lambda; 0)$ related by the central symmetry with respect to $p_0 = 0$. This symmetry is an isometry preserving the lattice Λ and the distances $d_0 < d_1 < \dots < d_n$. Making a choice by this inevitable ambiguity, we uniquely identify a point $q \in (S - 0) \cap V(\Lambda; 0)$ relative to the already fixed lattice Λ .

If the matrix $\text{PDD}(S; k)$ has $m \geq 3$ rows, any further point $p \in (S - \{0, q\}) \cap V(\Lambda; 0)$ will be uniquely determined as follows. Similarly to the point q above, we extract $n + 1$ shortest distances from the third row. In addition to $p_0 = 0$, we look for other n nearest neighbors that have specified distances to a next point p . Since the second point q is already fixed, the third point p is also restricted by the distance $|p - q|$ appearing once only in the second and third rows of $\text{PDD}(S; k)$. This distance doesn't help to resolve the ambiguity between $\pm p$ only q belongs to the bisector of points equidistant to $\pm p$. In this case the points $p, 0, q$ form a right-angle triangle, which is forbidden by condition (8a). Hence p and any further point of $S \cap V(\Lambda; 0)$ is uniquely determined by the fixed lattice Λ and second point q . ◀

Lemmas 14, 15 and a few auxiliary concepts below are needed to prove Theorem 10.

The volume of the unit ball in \mathbb{R}^n is $V_n = \frac{\pi^{n/2}}{\Gamma(\frac{n}{2} + 1)}$, where Γ denotes Euler's Gamma function $\Gamma(m) = (m - 1)!$ and $\Gamma(\frac{m}{2} + 1) = \sqrt{\pi}(m - \frac{1}{2})(m - \frac{3}{2}) \dots \frac{1}{2}$ for any integer $m \geq 1$.

The *Point Packing Coefficient* is $c(S) = \sqrt[n]{\frac{\text{Vol}[U]}{mV_n}}$, where a cell U may not be primitive since $\frac{\text{Vol}[U]}{m}$ is independent of U . Then $(c(S))^n$ is inversely proportional to the density of S , where every point has the mass V_n . The *diameter* of a unit cell U is $d = \sup_{a, b \in U} |a - b|$.

► **Lemma 14 (bounds on points within a ball).** Let $S \subset \mathbb{R}^n$ be any periodic point set with a unit cell U , which generates a lattice Λ and has a diameter d . For any point $p \in S \cap U$ and a radius r , consider the *lower union* $U'(p; r) = \bigcup\{(U + \vec{v}) \mid \vec{v} \in \Lambda, (U + \vec{v}) \subset \bar{B}(p; r)\}$ and the *upper union* $U''(p; r) = \bigcup\{(U + \vec{v}) \mid \vec{v} \in \Lambda, (U + \vec{v}) \cap \bar{B}(p; r) \neq \emptyset\}$. Then the number of points from S in the closed ball $\bar{B}(p; r)$ with center p and radius r has the bounds $\left(\frac{r - d}{c(S)}\right)^n \leq m \frac{\text{Vol}[U'(p; r)]}{\text{Vol}[U]} \leq |S \cap \bar{B}(p; r)| \leq m \frac{\text{Vol}[U''(p; r)]}{\text{Vol}[U]} \leq \left(\frac{r + d}{c(S)}\right)^n$. ■

Proof. Intersect the three regions $U'(p; r) \subset \bar{B}(p; r) \subset U''(p; r)$ with S in \mathbb{R}^n and count the numbers of resulting points: $|S \cap U'(p; r)| \leq |S \cap \bar{B}(p; r)| \leq |S \cap U''(p; r)|$.

The union $U'(p; r)$ consists of $\frac{\text{Vol}[U'(p; r)]}{\text{Vol}[U]}$ cells, which all have the same volume $\text{Vol}[U]$. Since $|S \cap U| = m$, we now get $|S \cap U'(p; r)| = m \frac{\text{Vol}[U'(p; r)]}{\text{Vol}[U]}$. Similarly we count the points in the upper union: $|S \cap U''(p; r)| = m \frac{\text{Vol}[U''(p; r)]}{\text{Vol}[U]}$. The bounds of $|S \cap \bar{B}(p; r)|$ become

$$m \frac{\text{Vol}[U'(p; r)]}{\text{Vol}[U]} \leq |S \cap \bar{B}(p; r)| \leq m \frac{\text{Vol}[U''(p; r)]}{\text{Vol}[U]},$$

$$\text{Vol}[U'(p; r)] \leq \frac{\text{Vol}[U]}{m} |S \cap \bar{B}(p; r)| \leq \text{Vol}[U''(p; r)].$$

716 For the diameter d of the unit cell U , the smaller ball $\bar{B}(p; r - d)$ is completely contained
 717 within the lower union $U'(p; r)$. Indeed, if $|\vec{q} - \vec{p}| \leq r - d$, then $q \in U + \vec{v}$ for some $\vec{v} \in \Lambda$.
 718 Then $(U + \vec{v})$ is covered by the ball $\bar{B}(q; d)$, hence by $\bar{B}(p; r)$ due to the triangle inequality.

The inclusion $\bar{B}(p; r - d) \subset U'(p; r)$ implies the lower bound for the volumes:

$$V_n(r - d)^n = \text{Vol}[\bar{B}(p; r - d)] \leq \text{Vol}[U'(p; r)] \text{ where,}$$

V_n is the volume of the unit ball in \mathbb{R}^n . The similar inclusion $U''(p; r) \subset \bar{B}(p; r + d)$ gives

$$\text{Vol}[U''(p; r)] \leq \text{Vol}[\bar{B}(p; r + d)] = V_n(r + d)^n, \quad V_n(r - d)^n \leq \frac{\text{Vol}[U]}{m} |S \cap B(p; r)| \leq V_n(r + d)^n,$$

719 $\frac{mV_n}{\text{Vol}[U]}(r - d)^n \leq |S \cap B(p; r)| \leq \frac{mV_n}{\text{Vol}[U]}(r + d)^n$, which implies the required inequality. ◀

720 ▶ **Lemma 15** (distance bounds). Let $S \subset \mathbb{R}^n$ be any periodic point set with a unit cell U of
 721 diameter d . For any motif point $p \in M = S \cap U$, let $d_k(S; p)$ be the distance from p to its
 722 k -th nearest neighbour in S . Then $c(S) \sqrt[n]{k} - d < d_k(S; p) \leq c(S) \sqrt[n]{k} + d$ for any $k \geq 1$. ■

723 **Proof.** The closed ball $\bar{B}(p; r)$ of radius $r = d_k(S; p)$ has more than k points (including p) from
 724 S . The upper bound of Lemma 14 for $r = d_k(S; p)$ implies that $k < |S \cap \bar{B}(p; r)| \leq \frac{(r + d)^n}{(c(S))^n}$.

725 Taking the n -th root of both sides, we get $\sqrt[n]{k} < \frac{r + d}{c(S)}$, so $r = d_k(S; p) > c(S) \sqrt[n]{k} - d$.

726 For any smaller radius $r < d_k(S; p)$, the closed ball $\bar{B}(p; r)$ contains at most k points
 727 (including p) from S . The lower bound of Lemma 14 for any $r < d_k(S; p)$ implies that
 728 $\frac{(r - d)^n}{c(S)^n} \leq |S \cap \bar{B}(p; r)| \leq k$. Since $\frac{(r - d)^n}{c(S)^n} \leq k$ holds for the constant upper bound k and
 729 any radius $r < d_k(S; p)$, the same inequality holds for the radius $r = d_k(S; p)$.

730 Similarly to the upper bound above, we get $\frac{r - d}{c(S)} \leq \sqrt[n]{k}$, $r = d_k(S; p) \leq c(S) \sqrt[n]{k} + d$.

731 Combine the two bounds above as follows: $c(S) \sqrt[n]{k} - d < d_k(S; p) \leq c(S) \sqrt[n]{k} + d$. ◀

732 Define the *skewness* of a unit cell U with a diameter d as $\nu = \frac{d}{\sqrt[n]{\text{Vol}[U]}}$. Most reduced
 733 cell U have a small ν , though in \mathbb{R}^2 the rectangular cell with edge-lengths $1, l$ has $\nu =$
 734 $\sqrt{\frac{1 + l^2}{l}} \rightarrow +\infty$ as $l \rightarrow +\infty$, though such cells are rare for real periodic structures.

735 **Full proof of Theorem 10 for $h = 1$.** Let the origin 0 be in the center of the unit cell U . If
 736 d is the diameter of U , any point $p \in M = S \cap U$ is covered by the closed ball $\bar{B}(0, 0.5d)$.

By Lemma 15 all k neighbours of p are covered by the ball $\bar{B}(0; r)$ of radius $r = c(S) \sqrt[n]{k} + 1.5d$. To generate all Λ -translates of M within $\bar{B}(0; r)$, we gradually extend U in spherical layers by adding more shifted cells until we get the upper union $U''(0; r) \supset \bar{B}(0; r)$. By Lemma 14 the union $U''(0; r)$ includes k neighbors of motif points and has at most $\mu =$

$$= m \frac{\text{Vol}[U''(0; r)]}{\text{Vol}[U]} \leq \left(\frac{c(S) \sqrt[n]{k} + 2.5d}{c(S)} \right)^n = \left(\sqrt[n]{k} + \frac{2.5d}{c(S)} \right)^n = O(2^n (k + m(2.5\nu)^n V_n)) \text{ points.}$$

737 To get the last expression, we use the rough estimate $(a+b)^n \leq 2^n(a^n + b^n)$ with $a^n = k$ and
 738 $b^n = \left(\frac{2.5d}{c(S)}\right)^n = \frac{(2.5d)^n}{\text{Vol}[U]} m V_n = m(2.5\nu)^n V_n$, where $\nu = \frac{d}{\sqrt[n]{\text{Vol}[U]}}$ is the skewness of U .

A cover tree on μ points can be built in time $O(\mu \log \mu)$ by [7, Theorems 4, 6]. Then all k neighbours of $m \leq \mu$ motif points $p \in M$ can be found in time $O(mk \log^2 k)$ by [19, chapter 3], which extends [13, Theorem 2] for $k = 1$. By Definition 3 we lexicographically sort m lists of ordered distances in time $O(km \log m)$, because a comparison of two ordered lists of the length k takes $O(k)$ time. These ordered lists are the rows of the matrix $D(S; k)$. Then identical rows are collapsed to a single row with in time $O(km)$. Using $\log \mu = n \log 2 + O(\log(k + m(2.5\nu)^n V_n)) = nO(\log(km))$, PDD($S; k$) is found in total time

$$O(\mu \log \mu + mk \log^2 k) = O(2^n(k + m(2.5\nu)^n V_n)n \log(km) + mk \log^2 k) =$$

739 $= O((5\nu)^n V_n km \log m \log^2 k)$, which is near linear in both key inputs k, m . ◀

740 Our implementations of PDD^{h} invariants in Python uses the n -d tree [10] on μ points in
 741 \mathbb{R}^n , which performs faster in small dimensions than a cover tree but has no proved complexity
 742 for a nearest neighbour search.

743 **Full proof of Theorem 10 for $h > 1$.** We might need up to $k + h - 1$ neighbors for each
 744 $p \in M$, because up to $h - 1$ neighbors of p can belong to a subset A of h points including p_i .

745 For any subset $A \subset S$ of $h > 1$ points, all distances in the corresponding row of
 746 PDD^{h}($S; k$) were already computed for PDD($S; k$). Indeed, for any point $p_i \in A$, we add
 747 its k nearest neighbors (together with distances to p_i) to the pool of neighbors for all points
 748 of A . For every point of this pool, we build a list of ordered distances to all points of A in a
 749 time $O(h \log h)$. Since the pool has at most hk points, we lexicographically order the lists
 750 of the length h in time $O(h^2 k \log(hk))$. Hence a single row of PDD^{h}($S; k$) is completed
 751 in the extra time $O(h^2 k \log(hk))$. Since there are $O(m^h)$ rows corresponding to unordered
 752 subsets $A \subset S$ of h points, all rows will be complete in time $O(h^2 km^h \log(hk))$.

753 It remains to order $O(m^h)$ rows of the length k (with each component of size h) in time
 754 $O(hkm^h \log m)$. Hence the total time for PDD^{h} is $O(h^2 km^h (5\nu)^n V_n \log(hm) \log^2 k)$. ◀

755 **C Appendix C: computations of Pointwise Distance Distributions**

756 This appendix shows that PDD^{2} distinguishes pairs of finite sets in [33, Figure S4(A,B,C)],
 757 which were impossible to distinguish up to isometry by past distance-based invariants.

758 ▶ **Example 16** (5-point sets). The 5-point sets in Fig. 6 have pairwise distances in Table 4.

distances of S_-	R_-	R_+	G_-	G_+	B_-	distances of S_+	R_-	R_+	G_-	G_+	B_+
$R_-(-2, 0, -2)$	0	$\sqrt{32}$	$\sqrt{6}$	$\sqrt{14}$	$\sqrt{6}$	$R_-(-2, 0, -2)$	0	$\sqrt{32}$	$\sqrt{6}$	$\sqrt{14}$	$\sqrt{14}$
$R_+(+2, 0, +2)$	$\sqrt{32}$	0	$\sqrt{14}$	$\sqrt{6}$	$\sqrt{14}$	$R_+(+2, 0, +2)$	$\sqrt{32}$	0	$\sqrt{14}$	$\sqrt{6}$	$\sqrt{6}$
$G_-(-1, -1, 0)$	$\sqrt{6}$	$\sqrt{14}$	0	$\sqrt{8}$	$\sqrt{6}$	$G_-(-1, -1, 0)$	$\sqrt{6}$	$\sqrt{14}$	0	$\sqrt{8}$	$\sqrt{6}$
$G_+(+1, +1, 0)$	$\sqrt{14}$	$\sqrt{6}$	$\sqrt{8}$	0	$\sqrt{2}$	$G_+(+1, +1, 0)$	$\sqrt{14}$	$\sqrt{6}$	$\sqrt{8}$	0	$\sqrt{2}$
$B_-(0, +1, -1)$	$\sqrt{6}$	$\sqrt{14}$	$\sqrt{6}$	$\sqrt{2}$	0	$B_+(0, +1, +1)$	$\sqrt{14}$	$\sqrt{6}$	$\sqrt{6}$	$\sqrt{2}$	0

■ **Table 4** The matrix of pairwise distances between all points of the 5-point set S_{\pm} in Fig. 6.

S_- distances to	1st	2nd	3rd	4th	S_+ distances to	1st	2nd	3rd	4th
$R_- = (-2, 0, -2)$	$\sqrt{6}$	$\sqrt{6}$	$\sqrt{14}$	$\sqrt{32}$	$R_- = (-2, 0, -2)$	$\sqrt{6}$	$\sqrt{14}$	$\sqrt{14}$	$\sqrt{32}$
$R_+ = (+2, 0, +2)$	$\sqrt{6}$	$\sqrt{14}$	$\sqrt{14}$	$\sqrt{32}$	$R_+ = (+2, 0, +2)$	$\sqrt{6}$	$\sqrt{14}$	$\sqrt{14}$	$\sqrt{32}$
$G_- = (-1, -1, 0)$	$\sqrt{6}$	$\sqrt{6}$	$\sqrt{8}$	$\sqrt{14}$	$G_- = (-1, -1, 0)$	$\sqrt{6}$	$\sqrt{6}$	$\sqrt{8}$	$\sqrt{14}$
$G_+ = (+1, +1, 0)$	$\sqrt{2}$	$\sqrt{6}$	$\sqrt{8}$	$\sqrt{14}$	$G_+ = (+1, +1, 0)$	$\sqrt{2}$	$\sqrt{6}$	$\sqrt{8}$	$\sqrt{14}$
$B_- = (0, +1, -1)$	$\sqrt{2}$	$\sqrt{6}$	$\sqrt{6}$	$\sqrt{14}$	$B_+ = (0, +1, -1)$	$\sqrt{2}$	$\sqrt{6}$	$\sqrt{6}$	$\sqrt{14}$

■ **Table 5** For each point from S_{\mp} in Fig. 6, the distances from Table 4 are ordered in each row.

Table 5 illustrates Definition 3 of PDD for the sets S_{\pm} in Fig. 6 and confirm that

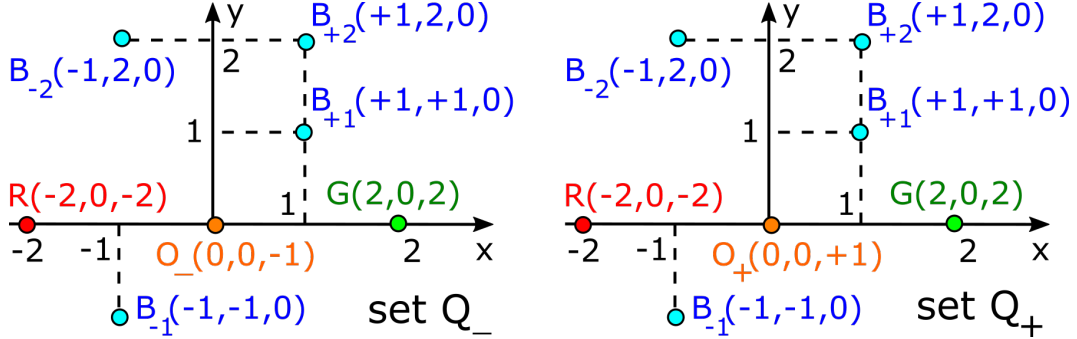
$$\text{PDD}(S_-; 4) = \begin{pmatrix} 1/5 & \sqrt{2} & \sqrt{6} & \sqrt{6} & \sqrt{14} \\ 1/5 & \sqrt{2} & \sqrt{6} & \sqrt{8} & \sqrt{14} \\ 1/5 & \sqrt{6} & \sqrt{6} & \sqrt{8} & \sqrt{14} \\ 1/5 & \sqrt{6} & \sqrt{6} & \sqrt{14} & \sqrt{32} \\ 1/5 & \sqrt{6} & \sqrt{14} & \sqrt{14} & \sqrt{32} \end{pmatrix} = \text{PDD}(S_+; 4).$$

pair in S_-	dist.	dist. pair to neighb.1	dist. pair to neighb.2	dist. pair to neighb.3
$\{R_-, R_+\}$	$\sqrt{32}$	$(\sqrt{6}, \sqrt{14})$	$(\sqrt{6}, \sqrt{14})$	$(\sqrt{6}, \sqrt{14})$
$\{R_-, G_-\}$	$\sqrt{6}$	$(\sqrt{6}, \sqrt{6})$	$(\sqrt{8}, \sqrt{14})$	$(\sqrt{14}, \sqrt{32})$
$\{R_-, G_+\}$	$\sqrt{14}$	$(\sqrt{2}, \sqrt{6})$	$(\sqrt{6}, \sqrt{8})$	$(\sqrt{6}, \sqrt{32})$
$\{R_-, B_-\}$	$\sqrt{6}$	$(\sqrt{2}, \sqrt{14})$	$(\sqrt{6}, \sqrt{6})$	$(\sqrt{14}, \sqrt{32})$
$\{R_+, G_-\}$	$\sqrt{14}$	$(\sqrt{6}, \sqrt{8})$	$(\sqrt{6}, \sqrt{14})$	$(\sqrt{6}, \sqrt{32})$
$\{R_+, G_+\}$	$\sqrt{6}$	$(\sqrt{2}, \sqrt{14})$	$(\sqrt{8}, \sqrt{14})$	$(\sqrt{14}, \sqrt{32})$
$\{R_+, B_-\}$	$\sqrt{14}$	$(\sqrt{2}, \sqrt{6})$	$(\sqrt{6}, \sqrt{14})$	$(\sqrt{6}, \sqrt{32})$
$\{G_-, G_+\}$	$\sqrt{8}$	$(\sqrt{2}, \sqrt{6})$	$(\sqrt{6}, \sqrt{14})$	$(\sqrt{6}, \sqrt{14})$
$\{G_-, B_-\}$	$\sqrt{6}$	$(\sqrt{2}, \sqrt{8})$	$(\sqrt{6}, \sqrt{6})$	$(\sqrt{14}, \sqrt{14})$
$\{G_+, B_-\}$	$\sqrt{2}$	$(\sqrt{6}, \sqrt{8})$ to G_-	$(\sqrt{6}, \sqrt{14})$ to R_-	$(\sqrt{6}, \sqrt{14})$ to R_+
pair in S_+	dist.	dist. pair to neighb.1	dist. pair to neighb.2	dist. pair to neighb.3
$\{R_-, R_+\}$	$\sqrt{32}$	$(\sqrt{6}, \sqrt{14})$	$(\sqrt{6}, \sqrt{14})$	$(\sqrt{6}, \sqrt{14})$
$\{R_-, G_-\}$	$\sqrt{6}$	$(\sqrt{6}, \sqrt{14})$	$(\sqrt{8}, \sqrt{14})$	$(\sqrt{14}, \sqrt{32})$
$\{R_-, G_+\}$	$\sqrt{14}$	$(\sqrt{2}, \sqrt{14})$	$(\sqrt{6}, \sqrt{8})$	$(\sqrt{6}, \sqrt{32})$
$\{R_-, B_+\}$	$\sqrt{14}$	$(\sqrt{2}, \sqrt{14})$	$(\sqrt{6}, \sqrt{6})$	$(\sqrt{6}, \sqrt{32})$
$\{R_+, G_-\}$	$\sqrt{14}$	$(\sqrt{6}, \sqrt{6})$	$(\sqrt{6}, \sqrt{8})$	$(\sqrt{6}, \sqrt{32})$
$\{R_+, G_+\}$	$\sqrt{6}$	$(\sqrt{2}, \sqrt{6})$	$(\sqrt{8}, \sqrt{14})$	$(\sqrt{14}, \sqrt{32})$
$\{R_+, B_+\}$	$\sqrt{6}$	$(\sqrt{2}, \sqrt{6})$	$(\sqrt{6}, \sqrt{14})$	$(\sqrt{14}, \sqrt{32})$
$\{G_-, G_+\}$	$\sqrt{8}$	$(\sqrt{2}, \sqrt{6})$	$(\sqrt{6}, \sqrt{14})$	$(\sqrt{6}, \sqrt{14})$
$\{G_-, B_+\}$	$\sqrt{6}$	$(\sqrt{2}, \sqrt{8})$	$(\sqrt{6}, \sqrt{14})$	$(\sqrt{6}, \sqrt{14})$
$\{G_+, B_+\}$	$\sqrt{2}$	$(\sqrt{6}, \sqrt{6})$ to R_+	$(\sqrt{6}, \sqrt{8})$ to G_-	$(\sqrt{14}, \sqrt{14})$ to R_-

■ **Table 6** For any unordered pair $\{p_i, p_j\} \subset S_{\mp}$ in Figure 6, each row includes the distance $|\vec{p}_i - \vec{p}_j|$ and lexicographically ordered pairs $|\vec{p}_i - \vec{p}_i| \leq |\vec{p}_j - \vec{p}_i|$ of distances from p_i, p_j to other $p_l \in S_{\mp}$. Both sets have one pair at distance $\sqrt{2}$ whose rows in $\text{PDD}^{\{2\}}$ differ by distances to neighbors 1,2,3.

759 The equality of the first order $\text{PDD}(S_-; 4) = \text{PDD}(S_+; 4)$ motivated us to introduce the
 760 stronger higher order $\text{PDD}^{\{h\}}$, which distinguish S_{\pm} already for $h = 2$ in Table 3, which
 761 might be easier to understand from intermediate Table 6 with highlighted differences. ■

762 ► **Example 17** (7-point sets). The sets Q_{\pm} in [33, Figure S4(B)] have distances in Table 7.
 763 Table 8 shows two pairs of the only rows in $\text{PDD}^{\{2\}}(Q_{\pm}; 3)$ starting from distance $\sqrt{6}$.
 764 The highlighted pairs of distances imply that $\text{PDD}^{\{2\}}(Q_-; k) \neq \text{PDD}^{\{2\}}(Q_+; k)$ for $k \geq 1$. ■



■ **Figure 7** **Left:** (x, y) -projection of the 7-point set $Q_- \subset \mathbb{R}^3$ consisting of the red point $R = (-2, 0, -2)$, green point $G = (2, 0, 2)$, four blue points $B_{\pm 1} = (\pm 1, \pm 1, 0)$, $B_{\pm 2} = (\pm 1, 2, 0)$ and orange point $O_- = (0, 0, -1)$. **Right:** to get the set $Q_+ \subset \mathbb{R}^3$ from Q_- , replace O_- by $O_+ = (0, 0, +1)$.

distances of Q_-	R	G	B_{-1}	B_{+1}	B_{-2}	B_{+2}	O_-
$R = (-2, 0, -2)$	0	$\sqrt{32}$	$\sqrt{6}$	$\sqrt{14}$	3	$\sqrt{17}$	$\sqrt{5}$
$G = (+2, 0, +2)$	$\sqrt{32}$	0	$\sqrt{14}$	$\sqrt{6}$	$\sqrt{17}$	3	$\sqrt{13}$
$B_{-1} = (-1, -1, 0)$	$\sqrt{6}$	$\sqrt{14}$	0	$\sqrt{8}$	3	$\sqrt{13}$	$\sqrt{3}$
$B_{+1} = (+1, +1, 0)$	$\sqrt{14}$	$\sqrt{6}$	$\sqrt{8}$	0	$\sqrt{5}$	1	$\sqrt{3}$
$B_{-2} = (-1, 2, 0)$	3	$\sqrt{17}$	3	$\sqrt{5}$	0	2	$\sqrt{6}$
$B_{+2} = (+1, 2, 0)$	$\sqrt{17}$	3	$\sqrt{13}$	1	2	0	$\sqrt{6}$
$O_- = (0, 0, -1)$	$\sqrt{5}$	$\sqrt{13}$	$\sqrt{3}$	$\sqrt{3}$	$\sqrt{6}$	$\sqrt{6}$	0

distances of Q_+	R	G	B_{-1}	B_{+1}	B_{-2}	B_{+2}	O_+
$R = (-2, 0, -2)$	0	$\sqrt{32}$	$\sqrt{6}$	$\sqrt{14}$	3	$\sqrt{17}$	$\sqrt{13}$
$G = (+2, 0, +2)$	$\sqrt{32}$	0	$\sqrt{14}$	$\sqrt{6}$	$\sqrt{17}$	3	$\sqrt{5}$
$B_{-1} = (-1, -1, 0)$	$\sqrt{6}$	$\sqrt{14}$	0	$\sqrt{8}$	3	$\sqrt{13}$	$\sqrt{3}$
$B_{+1} = (+1, +1, 0)$	$\sqrt{14}$	$\sqrt{6}$	$\sqrt{8}$	0	$\sqrt{5}$	1	$\sqrt{3}$
$B_{-2} = (-1, 2, 0)$	3	$\sqrt{17}$	3	$\sqrt{5}$	0	2	$\sqrt{6}$
$B_{+2} = (+1, 2, 0)$	$\sqrt{17}$	3	$\sqrt{13}$	1	2	0	$\sqrt{6}$
$O_+ = (0, 0, +1)$	$\sqrt{13}$	$\sqrt{5}$	$\sqrt{3}$	$\sqrt{3}$	$\sqrt{6}$	$\sqrt{6}$	0

■ **Table 7** The matrix of distances between all points of the 7-point set Q_{\pm} in [33, Figure S4(B)].

Q_- pair	dist.	dist. pair to neighb.1	dist. pair to neighb.2	dist. pair to neighb.3
$\{G, B_{+1}\}$	$\sqrt{6}$	(1, 3) to B_{+2}	$(\sqrt{3}, \sqrt{13})$ to O_-	$(\sqrt{8}, \sqrt{14})$ to B_{-1}
$\{R, B_{-1}\}$	$\sqrt{6}$	$(\sqrt{3}, \sqrt{5})$ to O_-	$(\sqrt{8}, \sqrt{14})$ to B_{+1}	(3, 3) to B_{-2}
Q_+ pair	dist.	dist. pair to neighb.1	dist. pair to neighb.2	dist. pair to neighb.3
$\{G, B_{+1}\}$	$\sqrt{6}$	(1, 3) to B_{+2}	$(\sqrt{3}, \sqrt{5})$ to O_+	$(\sqrt{8}, \sqrt{14})$ to B_{-1}
$\{R, B_{-1}\}$	$\sqrt{6}$	$(\sqrt{3}, \sqrt{13})$ to O_+	$(\sqrt{8}, \sqrt{14})$ to B_{+1}	(3, 3) to B_{-2}

■ **Table 8** Both 7-point sets Q_{\mp} have only two pairs $\{G, B_{+1}\}$ and $\{R, B_{-1}\}$ at distance $\sqrt{6}$, whose rows in $\text{PDD}^{\{2\}}$ differ by distances from O_{\pm} to these pairs, hence $\text{PDD}^{\{2\}}(Q_-; 1) \neq \text{PDD}^{\{2\}}(Q_+; 1)$.

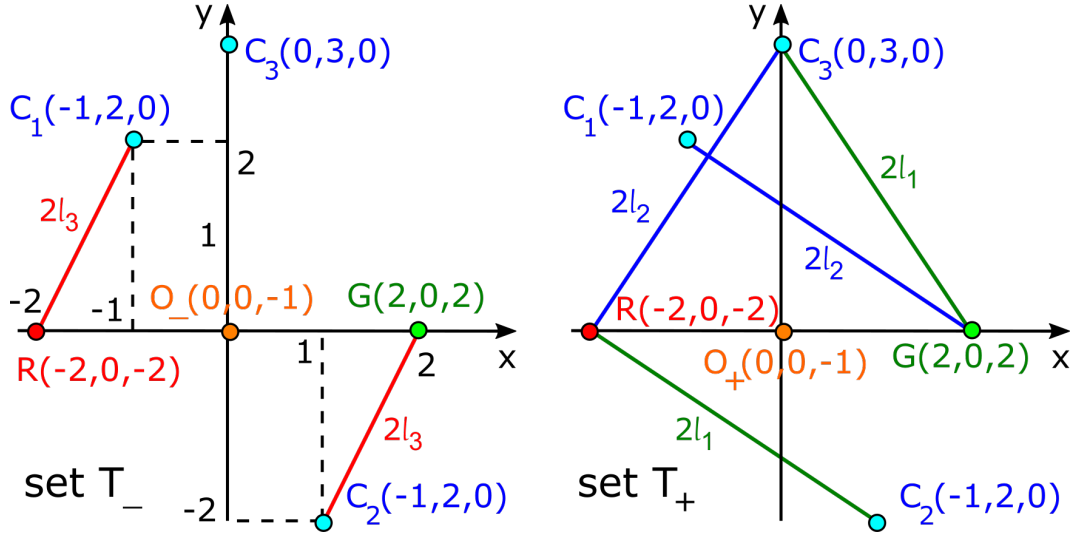


Figure 8 Left: (x, y) -projection of the 6-point set $T_- \subset \mathbb{R}^3$ consisting of the red point $R = (-2, 0, -2)$, green point $G = (2, 0, 2)$, three blue points $C_1 = (x_1, y_1, 0)$, $C_2 = (x_2, y_2, 0)$, $C_3 = (x_3, y_3, 0)$ and orange point $O_- = (0, 0, -1)$ so that $|RC_1| = 2l_3 = |GC_2|$, $|RC_2| = 2l_1 = |GC_3|$, $|RC_3| = 2l_2 = |GC_1|$. Right: to get the set $T_+ \subset \mathbb{R}^3$ from T_- , replace O_- by $O_+ = (0, 0, +1)$.

Example 18 (6-point sets). The sets T_{\pm} in [33, Figure S4(C)] have the points R, G, O_{\pm} from the sets Q_{\pm} in Example 17 and three new points $C_1(x_1, y_1, 0)$, $C_2(x_2, y_2, 0)$, $C_3(x_3, y_3, 0)$ such that $|RC_1| = |GC_2|$, $|RC_2| = |GC_3|$, $|RC_3| = |GC_1|$. Denote by $2l_1, 2l_2, 2l_3$ the lengths of the above line segments after their projection to the xy -plane so that

$$(x_2 + 2)^2 + y_2^2 = |RC_2|^2 - 4 = (2l_1)^2 = |GC_3|^2 - 4 = (x_3 - 2)^2 + y_3^2, \quad (18_1)$$

$$(x_3 + 2)^2 + y_3^2 = |RC_3|^2 - 4 = (2l_2)^2 = |GC_1|^2 - 4 = (x_1 - 2)^2 + y_1^2, \quad (18_2)$$

$$(x_1 + 2)^2 + y_1^2 = |RC_1|^2 - 4 = (2l_3)^2 = |GC_2|^2 - 4 = (x_2 - 2)^2 + y_2^2. \quad (18_3)$$

765 Comparing the left hand side of (18₁) with the right hand side of (18₃), we get $(2l_1)^2 - 4x_2 =$
 766 $(2l_3)^2 + 4x_2$, so $x_2 = \frac{l_1^2 - l_3^2}{2}$. Similarly, $x_3 = \frac{l_2^2 - l_1^2}{2}$, $x_1 = \frac{l_3^2 - l_2^2}{2}$ so that $x_1 + x_2 + x_3 = 0$.

767 From the right hand side of (18₂), we get $x_1^2 - 4x_1 + 4 + y_1^2 = 4l_2^2$, so $|O_{\pm}C_1|^2 = x_1^2 + y_1^2 + 1 =$
 768 $4l_2^2 + 4x_1 - 3 = 2l_2^2 + 2l_3^2 - 3$, similarly $|O_{\pm}C_2|^2 = 2l_3^2 + 2l_1^2 - 3$, $|O_{\pm}C_3|^2 = 2l_1^2 + 2l_2^2 - 3$.

769 Table 9 contains all pairwise distances between points of T_{\pm} . Then $\text{PDD}^{\{2\}}(T_{\pm}; 4)$ have
 770 equal rows corresponding to pairs $\{R, G\}, \{O_{\pm}, C_i\}, \{C_i, C_j\}$ for distinct $i, j = 1, 2, 3$. For
 771 example, in both $\text{PDD}^{\{2\}}(T_{\pm}; 4)$ the row of $\{R, G\}$ starts with their distance $\sqrt{32}$ and then
 772 include the same four pairs $(\sqrt{5}, \sqrt{13}), (2\sqrt{l_i^2 + 1}, 2\sqrt{l_{i-1}^2 + 1})$ for $i \in \{1, 2, 3\}$ modulo 3,
 773 which should be ordered and written lexicographically. Hence it makes sense to compare
 774 $\text{PDD}^{\{2\}}(T_{\pm}; 4)$ only by the remaining rows $\{R, O_{\pm}\}, \{G, O_{\pm}\}, \{R, C_i\}, \{G, C_j\}$ in Table 10.

775 Without loss of generality assume that $l_1 \geq l_2 \geq l_3$. If all the parameters are distinct,
 776 then $l_1 > l_2 > l_3$. Then the rows for $\{R, O_{-}\}$ and $\{G, O_{+}\}$ differ in Table 10 even after
 777 ordering each pair so that a smaller distance precedes a larger one, and after writing all pairs
 778 in the lexicographic order. So $\text{PDD}^{\{2\}}(T_{-}; 4) \neq \text{PDD}^{\{2\}}(T_{+}; 4)$ unless two of l_i are equal.

distances of T_-	R	G	C_1	C_2	C_3	O_-
$R = (-2, 0, -2)$	0	$\sqrt{32}$	$2\sqrt{l_3^2 + 1}$	$2\sqrt{l_1^2 + 1}$	$2\sqrt{l_2^2 + 1}$	$\sqrt{5}$
$G = (+2, 0, +2)$	$\sqrt{32}$	0	$2\sqrt{l_2^2 + 1}$	$2\sqrt{l_3^2 + 1}$	$2\sqrt{l_1^2 + 1}$	$\sqrt{13}$
$C_1 = (x_1, y_1, 0)$	$2\sqrt{l_3^2 + 1}$	$2\sqrt{l_2^2 + 1}$	0	$ C_1C_2 $	$ C_3C_1 $	$\sqrt{2l_2^2 + 2l_3^2 - 3}$
$C_2 = (x_2, y_2, 0)$	$2\sqrt{l_1^2 + 1}$	$2\sqrt{l_3^2 + 1}$	$ C_1C_2 $	0	$ C_2C_3 $	$\sqrt{2l_3^2 + 2l_1^2 - 3}$
$C_3 = (x_3, y_3, 0)$	$2\sqrt{l_2^2 + 1}$	$2\sqrt{l_1^2 + 1}$	$ C_3C_1 $	$ C_2C_3 $	0	$\sqrt{2l_1^2 + 2l_2^2 - 3}$
$O_- = (0, 0, -1)$	$\sqrt{5}$	$\sqrt{13}$	$\sqrt{2l_2^2 + 2l_3^2 - 3}$	$\sqrt{2l_3^2 + 2l_1^2 - 3}$	$\sqrt{2l_1^2 + 2l_2^2 - 3}$	0

distances of T_+	R	G	C_1	C_2	C_3	O_+
$R = (-2, 0, -2)$	0	$\sqrt{32}$	$2\sqrt{l_3^2 + 1}$	$2\sqrt{l_1^2 + 1}$	$2\sqrt{l_2^2 + 1}$	$\sqrt{13}$
$G = (+2, 0, +2)$	$\sqrt{32}$	0	$2\sqrt{l_2^2 + 1}$	$2\sqrt{l_3^2 + 1}$	$2\sqrt{l_1^2 + 1}$	$\sqrt{5}$
$C_1 = (x_1, y_1, 0)$	$2\sqrt{l_3^2 + 1}$	$2\sqrt{l_2^2 + 1}$	0	$ C_1C_2 $	$ C_3C_1 $	$\sqrt{2l_2^2 + 2l_3^2 - 3}$
$C_2 = (x_2, y_2, 0)$	$2\sqrt{l_1^2 + 1}$	$2\sqrt{l_3^2 + 1}$	$ C_1C_2 $	0	$ C_2C_3 $	$\sqrt{2l_3^2 + 2l_1^2 - 3}$
$C_3 = (x_3, y_3, 0)$	$2\sqrt{l_2^2 + 1}$	$2\sqrt{l_1^2 + 1}$	$ C_3C_1 $	$ C_2C_3 $	0	$\sqrt{2l_1^2 + 2l_2^2 - 3}$
$O_+ = (0, 0, +1)$	$\sqrt{13}$	$\sqrt{5}$	$\sqrt{2l_2^2 + 2l_3^2 - 3}$	$\sqrt{2l_3^2 + 2l_1^2 - 3}$	$\sqrt{2l_1^2 + 2l_2^2 - 3}$	0

■ **Table 9** The matrix of distances between all points of the 7-point set T_{\pm} in [33, Figure S4(C)].

779 If (say) $l_1 = l_2$, the lexicographically ordered rows of $\{R, O_-\}$ and $\{G, O_+\}$ coincide in
780 $\text{PDD}^{\{2\}}(T_{\pm}; 4)$, similarly the rows of $\{G, O_-\}$ and $\{R, O_+\}$. Hence it suffices to compare
781 only the six rows for the remaining pairs $\{R, C_i\}, \{G, C_j\}$ in $\text{PDD}^{\{2\}}(T_{\pm}; 4)$.

782 For $l_1 = l_2$, we get $x_3 = \frac{l_2^2 - l_1^2}{2} = 0$ and $x_1 = -x_2 = \frac{l_3^2 - l_2^2}{2}$. In equation (18₃) the
783 equality $(x_1 + 2)^2 + y_1^2 = (x_2 - 2)^2 + y_2^2$ with $x_1 = -x_2$ implies that $y_1^2 = y_2^2$. The even more
784 degenerate case $l_1 = l_2 = l_3$, means that $x_1 = x_2 = x_3 = 0$ and $y_1^2 = y_2^2 = y_3^2$, hence at least
785 two of C_1, C_2, C_3 should coincide. The above contradiction means that it remains to consider
786 only the case $l_1 = l_2 > l_3$ when $x_1 = -x_2 \neq 0 = x_3$ and $y_1 = \pm y_2$, see Fig. 8.

787 If $y_1 = y_2$, the sets T_{\pm} are isometric by $(x, y, z) \mapsto (-x, y, -z)$. If $y_1 = -y_2$ and
788 $y_3 = 0$, the sets T_{\pm} are isometric by $(x, y, z) \mapsto (-x, -y, -z)$. If $y_1 = -y_2$ and $y_3 \neq 0$, then
789 $C_1 = (x_1, y_1, 0)$, $C_2 = (-x_1, -y_1, 0)$, $C_3 \neq (0, 0, 0)$. In this case among the six remaining rows,
790 only the rows of $\{R, C_1\}, \{G, C_2\}$ have points at the distance $2\sqrt{l_3^2 + 1}$, see Table 10 for $i = 3$
791 considered modulo 3. Then $i + 1 \equiv 1 \pmod{3}$, $i - 1 \equiv 2 \pmod{3}$, so $l_{i+1} = l_1 = l_2 = l_{i-1}$.

792 Looking at the rows of $\{R, C_1\}, \{G, C_2\}$, the three common pairs in each of $\text{PDD}^{\{2\}}(T_{\pm}; 4)$
793 include the same distance $2\sqrt{l_1^2 + 1} = 2\sqrt{l_2^2 + 1}$ but differ by $|C_{i-1}C_i| = |C_2C_3| \neq |C_3C_1| =$
794 $|C_iC_{i+1}|$ since $C_1 = \pm C_2$, $C_3 \neq (0, 0, 0)$. This couple of different rows implies that
795 $\text{PDD}^{\{2\}}(T_-; 4) \neq \text{PDD}^{\{2\}}(T_+; 4)$ due to the swapped distances $\sqrt{5}, \sqrt{13}$ in their remaining
796 pairs, see Table 10 for the sets T_{\pm} in Fig. 8 with $l_1 = l_2 = \frac{\sqrt{13}}{2}$, $l_3 = \frac{\sqrt{5}}{2}$. ■

797 D Appendix D: breakthrough visualizations of large crystal datasets

798 This section explains visualisations of large crystal datasets for experts in applications.

799 A Crystallographic Information File (CIF) is typically used to represent 3D structures
800 of periodic crystals. The geometric part of CIF represents a unit cell (a parallelepiped)
801 $U \subset \mathbb{R}^3$ canonically by three edge-lengths a, b, c and between angles α, β, γ so that α is
802 between b, c opposite to a and so on. A CIF also contains a list of atoms, each with their
803 chemical element and three coordinates x, y, z (called *fractional*) of their atomic center. An
804 atom then Cartesian coordinates given by $x\vec{v}_1 + y\vec{v}_2 + z\vec{v}_3$ for the basis vectors $\vec{v}_1, \vec{v}_2, \vec{v}_3$

T_- pair	distance	common pairs in $\text{PDD}^{\{2\}}(T_{\pm}; 4)$	pairs that differ in $\text{PDD}^{\{2\}}(T_{\pm}; 4)$
$\{R, O_-\}$	$\sqrt{5}$	$(\sqrt{13}, \sqrt{32})$ to G	$(2\sqrt{l_3^2 + 1}, \sqrt{2l_2^2 + 2l_3^2 - 3})$ to C_1 , $(2\sqrt{l_1^2 + 1}, \sqrt{2l_3^2 + 2l_1^2 - 3})$ to C_2 , $(2\sqrt{l_2^2 + 1}, \sqrt{2l_1^2 + 2l_2^2 - 3})$ to C_3
$\{G, O_-\}$	$\sqrt{13}$	$(\sqrt{5}, \sqrt{32})$ to R	$(2\sqrt{l_2^2 + 1}, \sqrt{2l_2^2 + 2l_3^2 - 3})$ to C_1 , $(2\sqrt{l_3^2 + 1}, \sqrt{2l_3^2 + 2l_1^2 - 3})$ to C_2 , $(2\sqrt{l_1^2 + 1}, \sqrt{2l_1^2 + 2l_2^2 - 3})$ to C_3
$\{R, C_{i+1}\}$	$2\sqrt{l_i^2 + 1}$	$(2\sqrt{l_{i-1}^2 + 1}, \sqrt{32})$ to G , $(2\sqrt{l_{i+1}^2 + 1}, C_{i+1}C_{i-1})$ to C_{i-1} , $(2\sqrt{l_{i-1}^2 + 1}, C_iC_{i+1})$ to C_i	$(\sqrt{5}, \sqrt{2l_{i-1}^2 + 2l_i^2 - 3})$ to O_-
$\{G, C_{i-1}\}$	$2\sqrt{l_i^2 + 1}$	$(2\sqrt{l_{i+1}^2 + 1}, \sqrt{32})$ to R , $(2\sqrt{l_{i-1}^2 + 1}, C_{i+1}C_{i-1})$ to C_{i+1} , $(2\sqrt{l_{i+1}^2 + 1}, C_{i-1}C_i)$ to C_i	$(\sqrt{13}, \sqrt{2l_i^2 + 2l_{i+1}^2 - 3})$ to O_-
T_+ pair	distance	common pairs in $\text{PDD}^{\{2\}}(T_{\pm}; 4)$	pairs that differ in $\text{PDD}^{\{2\}}(T_{\pm}; 4)$
$\{G, O_+\}$	$\sqrt{5}$	$(\sqrt{13}, \sqrt{32})$ to R	$(2\sqrt{l_2^2 + 1}, \sqrt{2l_2^2 + 2l_3^2 - 3})$ to C_1 , $(2\sqrt{l_3^2 + 1}, \sqrt{2l_3^2 + 2l_1^2 - 3})$ to C_2 , $(2\sqrt{l_1^2 + 1}, \sqrt{2l_1^2 + 2l_2^2 - 3})$ to C_3
$\{R, O_+\}$	$\sqrt{13}$	$(\sqrt{5}, \sqrt{32})$ to G	$(2\sqrt{l_3^2 + 1}, \sqrt{2l_2^2 + 2l_3^2 - 3})$ to C_1 , $(2\sqrt{l_1^2 + 1}, \sqrt{2l_3^2 + 2l_1^2 - 3})$ to C_2 , $(2\sqrt{l_2^2 + 1}, \sqrt{2l_1^2 + 2l_2^2 - 3})$ to C_3
$\{R, C_{i+1}\}$	$2\sqrt{l_i^2 + 1}$	$(2\sqrt{l_{i-1}^2 + 1}, \sqrt{32})$ to G , $(2\sqrt{l_{i+1}^2 + 1}, C_{i+1}C_{i-1})$ to C_{i-1} , $(2\sqrt{l_{i-1}^2 + 1}, C_iC_{i+1})$ to C_i	$(\sqrt{13}, \sqrt{2l_{i-1}^2 + 2l_i^2 - 3})$ to O_+
$\{G, C_{i-1}\}$	$2\sqrt{l_i^2 + 1}$	$(2\sqrt{l_{i+1}^2 + 1}, \sqrt{32})$ to R , $(2\sqrt{l_{i-1}^2 + 1}, C_{i+1}C_{i-1})$ to C_{i+1} , $(2\sqrt{l_{i+1}^2 + 1}, C_{i-1}C_i)$ to C_i	$(\sqrt{5}, \sqrt{2l_i^2 + 2l_{i+1}^2 - 3})$ to O_+

Table 10 For the sets T_{\pm} , the distributions $\text{PDD}^{\{2\}}(T_{\pm}; 4)$ can differ only in rows of the pairs $\{R, O_{\pm}\}, \{G, O_{\pm}\}, \{R, C_i\}, \{G, C_i\}$ shown above, where $i \in \{1, 2, 3\}$ is considered modulo 3 so that $1 - 1 \equiv 3 \pmod{3}$. In rows of corresponding pairs of points, some pairs of distances are the same in both $\text{PDD}^{\{2\}}(T_{\pm}; 4)$, but other pairs can differ. If parameters l_1, l_2, l_3 are pairwise distinct, the rows $\{R, O_-\}, \{G, O_+\}$ include three different pairs of distances, so $\text{PDD}^{\{2\}}(T_-; 4) \neq \text{PDD}^{\{2\}}(T_+; 4)$.

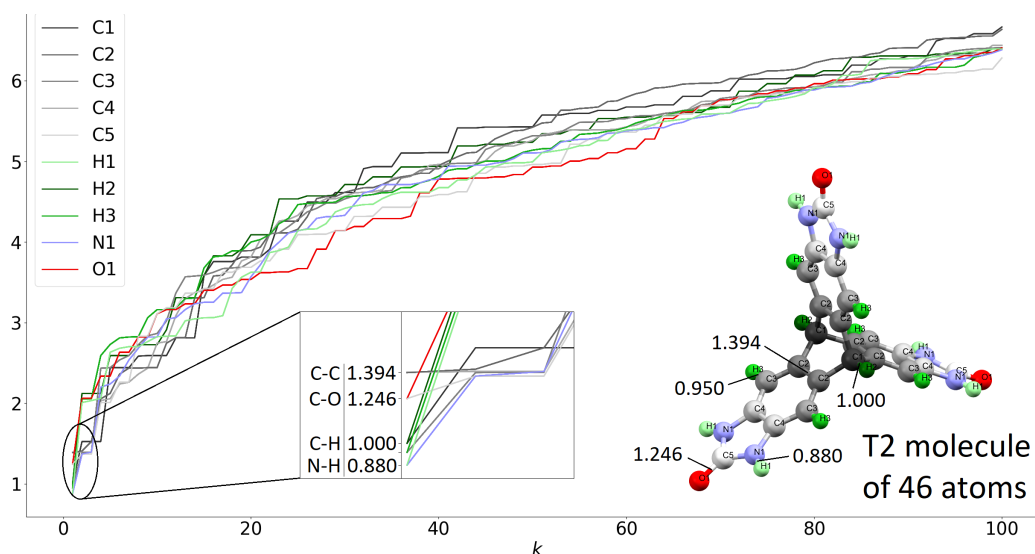
T_- pair	dist.	dist. to neighb.1	dist. to neighb.2	dist. to neighb.3	dist to neighb.4
$\{R, C_1\}$	3	$(\sqrt{2}, \sqrt{17})$ to C_3	$(\sqrt{5}, \sqrt{6})$ to O_-	$(\sqrt{17}, \sqrt{20})$ to C_2	$(\sqrt{17}, \sqrt{32})$ to G
$\{G, C_2\}$	3	$(\sqrt{6}, \sqrt{13})$ to O_-	$(\sqrt{17}, \sqrt{20})$ to C_1	$(\sqrt{17}, \sqrt{26})$ to C_3	$(\sqrt{17}, \sqrt{32})$ to R
T_+ pair	dist.	dist. to neighb.1	dist. to neighb.2	dist. to neighb.3	dist to neighb.4
$\{R, C_1\}$	3	$(\sqrt{2}, \sqrt{17})$ to C_3	$(\sqrt{6}, \sqrt{13})$ to O_+	$(\sqrt{17}, \sqrt{20})$ to C_2	$(\sqrt{17}, \sqrt{32})$ to G
$\{G, C_2\}$	3	$(\sqrt{5}, \sqrt{6})$ to O_+	$(\sqrt{17}, \sqrt{20})$ to C_1	$(\sqrt{17}, \sqrt{26})$ to C_3	$(\sqrt{17}, \sqrt{32})$ to R

Table 11 The above rows show that $\text{PDD}^{\{2\}}(T_-; 4) \neq \text{PDD}^{\{2\}}(T_+; 4)$ for the sets T_{\pm} with $C_1 = (-1, 2, 0)$, $C_2 = (1, -2, 0)$, $C_3 = (0, 3, 0)$ so that $l_1 = l_2 = \frac{\sqrt{5}}{2}$, $l_3 = \frac{\sqrt{13}}{2}$ in Table 10.

805 along edges of the unit cell U . In the paper we consider points without chemical labels,
806 however they can be easily added and taken into account when sorting rows of distances.

807 For the experimental crystal T2- ε , Fig. 9 shows 10 PDD curves corresponding to 10
808 types of non-isometric atomic positions within the T2 molecule. The rotation through 120°
809 around an axis keeps the T2 molecule and the whole infinite crystal T2- ε invariant, while the
810 three oxygen atoms shown in red simply rotate their positions. Hence all oxygen atom have

811 the same ordered distances to their neighbors and their PDD curves coincide. The same
 812 conclusion holds for six nitrogens whose positions are isometrically equivalent in T2.



■ **Figure 9** Each curve shows distances d_k from one atom of a T2 molecule to k -th neighbor in the T2- ε crystal. All 46 atoms split in 10 types: three oxygens form one type with the PDD curve in red, 23 carbons have 5 non-isometric positions in the molecule with PDD curves in 5 shades of gray. The zoomed part shows that PDD curves start from bond distances (in $\text{Å} = 10^{-10}$ m) between closest atoms and asymptotically behave like $\sqrt[3]{k}$.

813 Carbon atoms have five non-isometric positions, which generate five type of PDD curves
 814 in Fig. 9. All 10 PDD curves provide a finer classification of atomic types not only by
 815 chemical elements, but by their geometric positions within a molecule. For every atom, the
 816 first distance for $k = 1$ is the bond distance to its closest neighbor, see the zoomed beginnings
 817 of PDD curves. Though chemical elements can be included into the PDD matrix as an extra
 818 column, the above facts show that the PDD invariants can infer this chemistry.

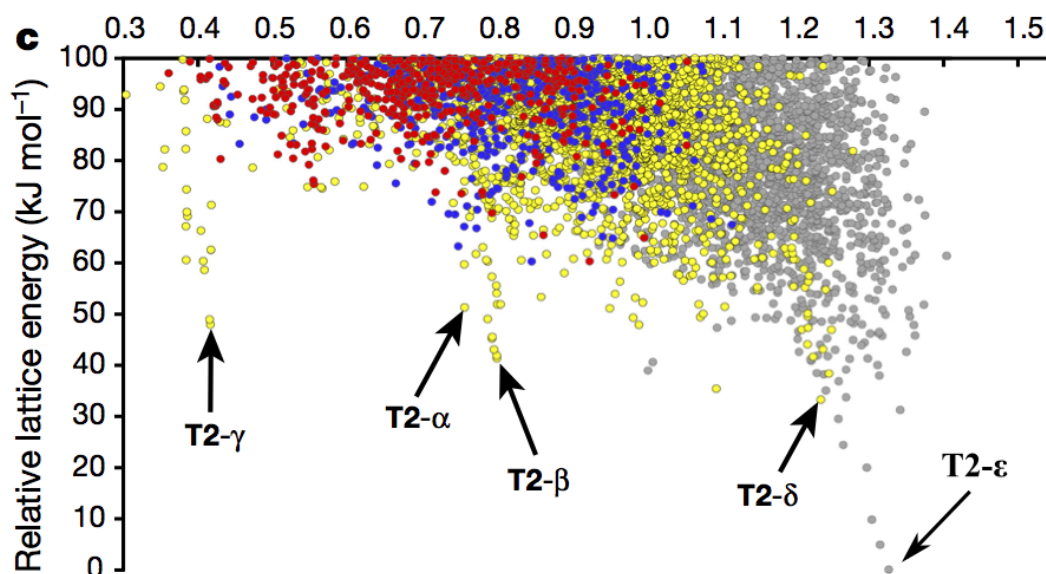
819 Our second dataset has all 12576 structures of crystalline drugs from the Cambridge
 820 Structural Database (CSD). Though CSD is the world's largest collection of more than 1.1M
 821 known crystals, it is basically a huge folder of Crystallographic Information Files (CIF) with
 822 limited search functions, for example by a chemical composition.

823 Though all crystalline drugs are based on many different molecules, these molecules tend
 824 to be smaller than the T2 molecule. Since larger than necessary values of k don't affect
 825 distances to closer neighbors, we tried $k = 100$ and $k = 200$ for the whole CSD drug subset.

826 After computing $\text{PDD}(S; k)$, we use a standard EMD algorithm for distances between
 827 these distributions. A Minimum Spanning Tree can be computed from a smaller graph on
 828 PDD invariants not requiring all pairwise distances. Since distances asymptotically approach
 829 $\text{PPC}(S)\sqrt[3]{k}$, we used the instantly computable Point Packing Coefficient $\text{PPC}(S)$ to find
 830 3000 neighbors for each of 12576 crystals. For $k = 200$, the computations of 12576×3000
 831 EMD distances (excluding all repetitions) took 7 hours 39 min (1.238 ms per comparison,
 832 2.19 sec per crystal). The time for PDD computations was in minutes. The time for drawing
 833 a Minimum Spanning Tree was in seconds.

834 A key challenge in visualization is to justifiably represent invariant data in a simple form.
 835 Past algorithms such as t-SNE [42], UMAP [28] are stochastic and can produce different
 836 outputs from repeated runs on the same input. Hence we used the more recent deterministic
 837 TreeMap [34] drawing a Minimum Spanning Tree (MST).

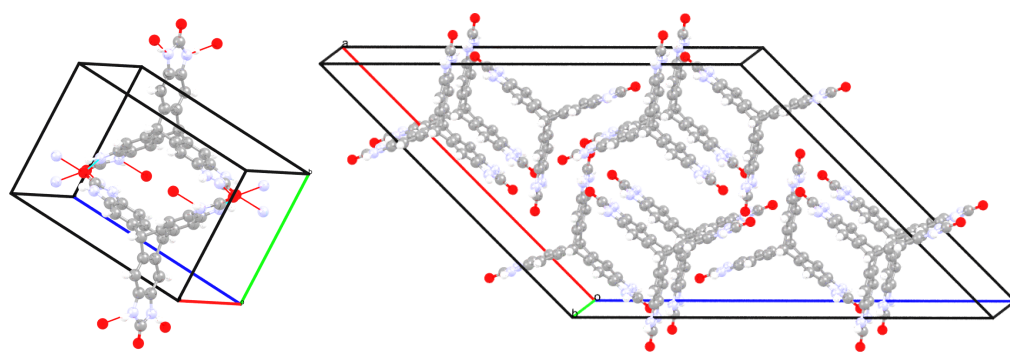
838 Informally, any MST can be considered as an optimal road network between cities. Such
 839 a network can be drawn in many different ways. Hence the most valuable and reliable new
 840 crystal data is in the new invariants $PDD^{\{h\}}$ and EMD distances between them, while MST
 841 is drawn only for visualization. Similarly, positions of cities and distances between them are
 842 more important than a sketch of a road network.



■ **Figure 10** State-of-the-art visualization of a CSP dataset, modified from Fig. 2d in [35]. Every predicted crystal has two coordinates (density, energy). The arrows show the predicted crystals that were manually matched to the five experimental crystals T2- α , T2- β , T2- γ , T2- δ , T2- ϵ .

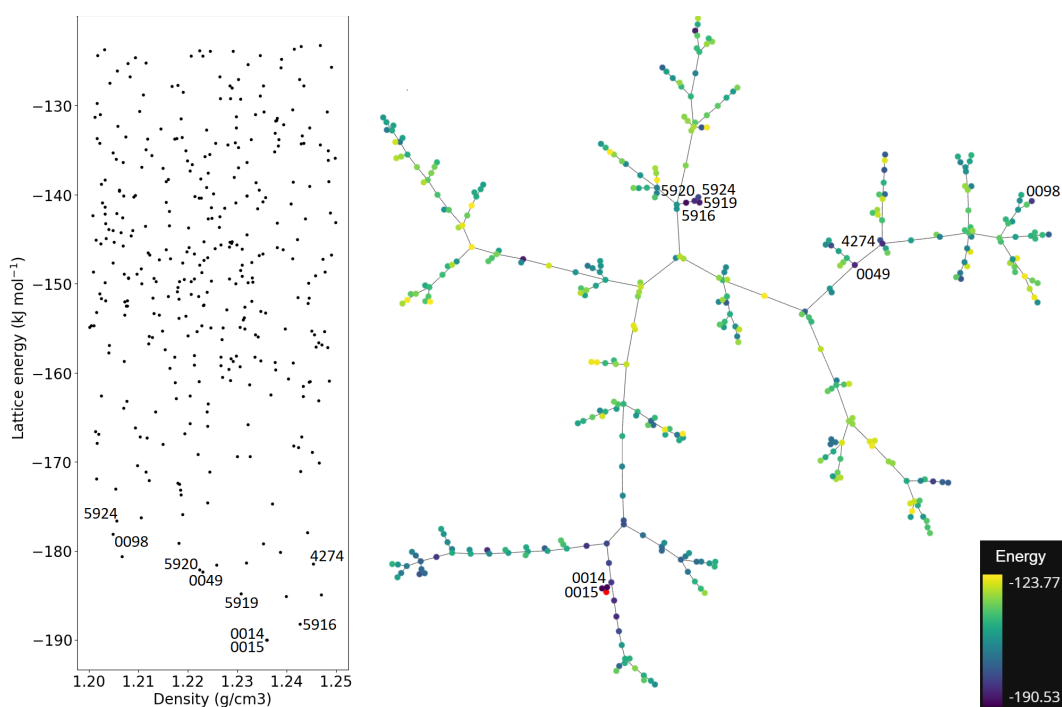
843 Fig. 12 illustrates key advantages of the invariant-based visualization in the right picture
 844 compared with the energy landscape in the left picture extracted from the state-of-the-art
 845 [35] in Fig. 10. Briefly, the MST based on stronger isometry invariants $PDD(S; 100)$ provides
 846 more information about crystal similarity than the cloud of points (density, energy). In the
 847 past, simulated versions were manually searched to match experimental crystals only by
 848 density. Measuring the energy of an experimental crystal needs an explosion disintegrating
 849 this crystal. For the experimental crystal T2- δ , dozens of simulated crystals were searched in
 850 the vertical strip in the left picture of Fig. 12. Simulated crystal 14 was visually chosen in
 851 [35] as the best match for T2- δ .

852 The new $PDD^{\{h\}}$ invariants can now automate the search for closest crystals, because
 853 $PDD^{\{h\}}$ can be computed for all types of simulated and experimental crystals. The MST in
 854 the right picture of Fig. 12 includes T2- δ as a red dot close to the near duplicate crystals
 855 14 and 15, which were not filtered out by past tools because of very different unit cells and
 856 motifs in Fig. 11. There were many other pairs of crystals with almost identical values of
 857 (density, energy), for example crystals 5920 and 0049, whose structures were found away from
 858 each other in the MST. When comparing this pair by the COMPACK algorithm, only one
 859 molecule is matched in Table 13. The resulting zero value of RMSD only means that crystals



■ **Figure 11** These crystals 14 and 15 based on the same T2 molecule have very different Crystallographic Information Files (with different motifs in unit cells of distinct shapes) but are nearly identical up to isometry.

860 5920 and 0049 are different (no similarity found), while EMD provides a proper distance.
 861 The right picture of Fig. 12 shows crystals 5920, 0049 in different branches of the MST.



■ **Figure 12 Left:** the vertical ‘strip’ of the energy landscape from Fig. 10 in the density range [1.2, 1.25] around the density of the experimental crystal T2- δ . The lowest energy crystals are highlighted by their IDs in the T2 dataset reported in [35]. **Right:** MST of the simulated crystals on the left plus the experimental crystal T2- δ in red, based on PDD(S ; 100). All simulated crystals are colored according to the energy bar in the bottom right corner.

862 The 4950 comparisons of 100 crystals by COMPACK took 3 hours 53 min (2.825 sec
 863 per comparison), which is 3 orders of magnitude slower than for EMD on PDD invariants.
 864 Table 12 says that over half the time (56%) only one molecule is matched, which means that
 865 no similarity was found between crystals based on identical molecules. Actually, 95% of the

# molecules	1	2	3	4	5	6	7	8	9	10	11	12	13	14	15
# comparisons	2784	1150	773	69	85	21	31	6	2	7	12	3	1	0	6

■ **Table 12** Outputs of the COMPACK algorithm [11] pairwise comparing 100 lowest energy crystals in the T2- δ ‘strip’ from Fig. 12. Most comparisons match only a small number of molecules.

■ **Table 13** The traditional COMPACK algorithm [11] measures packing similarity by attempting to match up to 15 (by default) molecules from two crystals. The low values 1,2,3 (of 15) mean that very few matches were found without a reliable Root Mean Square Deviation (RMSD).

	0014	0015	0049	0098	4274	5916	5919	5920	5924
0014	15	15	3	1	1	1	2	2	2
0015	15	15	3	1	1	1	2	2	2
0049	3	3	15	1	10	2	1	1	1
0098	1	1	1	15	1	1	1	1	1
4274	1	1	10	1	15	2	2	2	2
5916	1	1	2	1	2	15	10	10	10
5919	2	2	1	1	2	10	15	15	15
5920	2	2	1	1	2	10	15	15	15
5924	2	2	1	1	2	10	15	15	15

866 time, three or fewer molecules are matched, which is a failure to find also too small for the
 867 default number of 15 molecules. Rarely do matches exceed 10 (0.5%). Only 6 comparisons
 868 were 15/15 producing a more reliable packing similarity.

869 **The key contribution** is the new invariant data for edge-lengths of the MST, which
 870 can be visualized by TreeMap [34] or any other graph drawing algorithm. The continuity
 871 and invariance of higher order Pointwise Distance Distributions $PDD^{\{h\}}$ in Theorems 5 and
 872 7 guarantee than any crystal data analysis based on these invariants is justified.

873 Since a Minimum Spanning Tree has no cycles, some close crystals might appear at
 874 terminal vertices of distant branches, which could be connected to form a cycle. Drawing a
 875 graph with cycles will require more sophisticated algorithms. However, the new invariants
 876 can be used for a justifiable search of similar crystals without visualization.

877 We also have interactive versions of full Minimum Spanning Trees of the T2 dataset and
 878 CSD drug subset. In any Javascript-enabled browser one can zoom these TreeMaps, color
 879 the vertices by properties, hover over any vertex to get more information. Though aspirin
 880 and paracetamol are chemically different, their crystal structures are found in close branches
 881 confirming their similar properties.

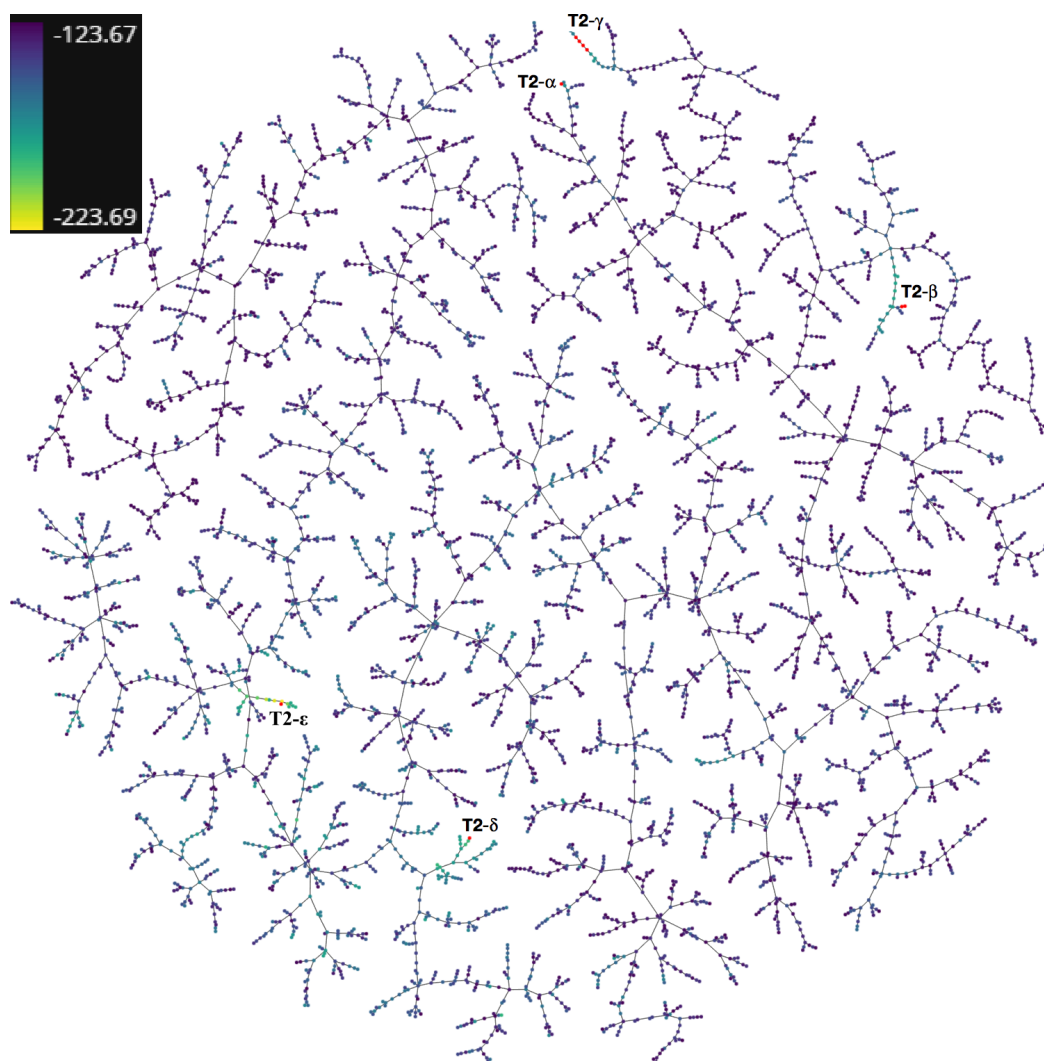
882 Our first dataset, T2, consists of 5679 simulated and 9 experimental crystals, all consisting
 883 of the same T2 molecules, those in Fig. 9. This dataset was reported in [35] in the new
 884 state-of-the-art approach to materials discovery through energy-structure maps.

885 This map or Crystal Structure Prediction (CSP) energy landscape is shown in Fig. 10,
 886 where every simulated crystal is represented by two coordinates (density, energy). The colors
 887 in Fig. 10 indicate a potential of a resulting crystalline material for methane adsorption.

888 The above ‘structure’ of a crystal was previously measured by only one continuous isometry
 889 invariant: the physical density equal to the weight of atoms within a unit cell, divided by
 890 the cell volume. All other descriptors are either non-invariants, e.g. powder diffraction

891 patterns depend on various thresholds and are not always reliable, or are discontinuous under
 892 perturbations, e.g. symmetry groups.

893 Fig. 13 is a substantial advancement in visualizing crystal datasets, because the underlying
 894 invariants $PDD(S; k)$ are much more informative than a single-value density. The nine
 895 experimental crystals (red dots) clearly split into five groups marked by T2- α , T2- β , T2- γ ,
 896 T2- δ , T2- ϵ . These nine experimental crystals have no known energies and cannot appear in
 897 the past energy landscapes. The four red dots at the very top represent slightly different
 898 forms of a T2- γ crystal synthesized at different temperatures.



■ **Figure 13** A Minimum Spanning Tree of 9+5679 T2 crystals drawn by TreeMap [34]. The distance between any crystals S, Q is the $EMD(PDD(S; 125), PDD(Q; 125))$. The color bar in the top left corner shows energy values. The minimum of -223.69 kJ/mol corresponds to 0 in Figure 10. Nine experimental crystals, which form the families T2- α , T2- β , T2- γ , T2- δ , T2- ϵ , are shown in red, because their energies are unknown.

899 The main contribution is replacing the single-value density by much stronger more
 900 isometry invariants $PDD^{\{h\}}$. Comparing crystals by only their densities was the latest

901 ‘state-of-the-art’ in [35], where 5 forms of 9 experimental crystals were initially matched to
902 dozens of simulated crystals with close densities. Then hundreds of crystals were visually
903 inspected to select the five matches in Fig. 10.

904 Now a ‘structure’ of a crystal can be much better represented by many more numerical
905 invariants in $PDD^{\{h\}}$. Fig. 13 is the first justified map of (a discretely sampled) space of
906 T2 crystals, because the underlying distance between $PDD^{\{h\}}$ invariants satisfies all metric
907 axioms and continuity under perturbations by [37] and Theorem 7.

908 The map in Fig. 13 shows a Minimum Spanning Tree built on 5679+9 crystals. Each
909 crystal is a vertex. The distance between any crystals is the Earth Mover’s distance between
910 the first order PDD invariants.

911 The most interesting vertices in the T2 map are experimental crystals shown in red,
912 because their energies are impractical to measure. The map shows experimental crystals
913 with simulated predictions for the first time, because past plots such as in Fig. 10 need all
914 energy values.

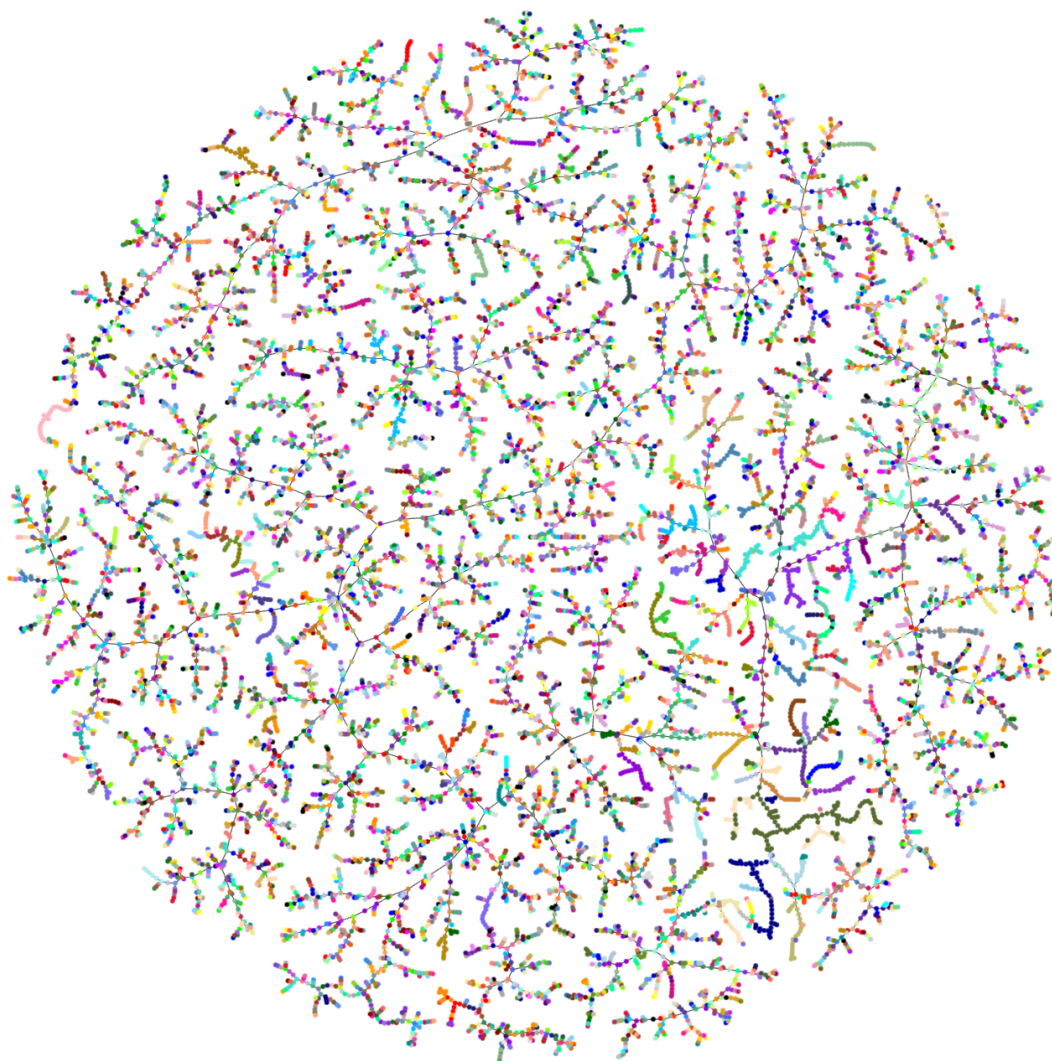
915 The maps can be interactively explored by opening the file T2L_PDD125_TMap.html
916 from the supplementary materials in any browser in the same folder with the corresponding
917 JavaScript files. In the interactive version one can color vertices by a property, which can be
918 changed in the drop-down menu in the bottom right corner. For example, all crystals with
919 low energies appear in yellow colors.

920 Fig. 14 show the much more diverse dataset of all 12576 crystalline drugs from the
921 Cambridge Structural Database (CSD). These crystals are manually split into 9234 families,
922 which are decided at the time of deposition. Usually, if several chemically identical crystals
923 are reported in the same paper, they get the 6-letter code in the CSD.

924 In Fig. 13 six of nine experimental T2 crystals have the codes DEBXIT01...06, though
925 they split into two subgroups: four nearly identical crystals T2- γ and two nearly identical
926 crystals T2- β . Our final experiment on all 229K molecular organic crystals found thousands
927 of such near duplicates in the Cambridge Structural Database.

928 — References —

- 929 1 Yonathan Aflalo, Alexander Bronstein, and Ron Kimmel. On convex relaxation of graph
930 isomorphism. *Proceedings of the National Academy of Sciences*, 112(10):2942–2947, 2015.
- 931 2 Helmut Alt, Kurt Mehlhorn, Hubert Wagener, and Emo Welzl. Congruence, similarity, and
932 symmetries of geometric objects. *Discrete & Computational Geometry*, 3:237–256, 1988.
- 933 3 LC Andrews, HJ Bernstein, and GA Pelletier. A perturbation stable cell comparison technique.
934 *Acta Crystallographica Section A*, 36(2):248–252, 1980.
- 935 4 Olga Anosova and Vitaliy Kurlin. Introduction to periodic geometry and topology.
936 *arXiv:2103.02749*, 2021.
- 937 5 Olga Anosova and Vitaliy Kurlin. An isometry classification of periodic point sets. In
938 *Proceedings of Discrete Geometry and Mathematical Morphology*, 2021.
- 939 6 Serge Belongie, Jitendra Malik, and Jan Puzicha. Shape matching and object recognition
940 using shape contexts. *Transactions PAMI*, 24(4):509–522, 2002.
- 941 7 Alina Beygelzimer, Sham Kakade, and John Langford. Cover trees for nearest neighbor. In
942 *Proceedings of ICML*, pages 97–104, 2006.
- 943 8 M. Bouniaev and N. Dolbilin. Regular and multi-regular t-bonded systems. *J. Information*
944 *Processing*, 25:735–740, 2017.
- 945 9 M. Boutin and G. Kemper. On reconstructing n-point configurations from the distribution of
946 distances or areas. *Advances in Applied Mathematics*, 32(4):709–735, 2004.



■ **Figure 14** A Minimum Spanning Tree of 12576 structures of all crystalline drugs in the Cambridge Structural Database. The distance between any crystals S, Q is the $\text{EMD}(\text{PDD}(S; 100), \text{PDD}(Q; 100))$. All structures from the same family are shown in one random color. This visualization is a breakthrough in understanding structure-property relationships of crystalline drugs: the world's largest pharmacy in a single image for the first time.

- 947 **10** Russell A. Brown. Building a balanced k -d tree in $o(kn \log n)$ time. *J. Computer Graphics*
948 *Techniques*, 4(1):50–68, 2015.
- 949 **11** J. Chisholm and S. Motherwell. Compack: a program for identifying crystal structure similarity
950 using distances. *J. Applied Crystallography*, 38(1):228–231, 2005.
- 951 **12** John Conway and Neil Sloane. Low-dimensional lattices. vi. voronoi reduction of three-
952 dimensional lattices. *Proceedings of the Royal Society A*, 436(1896):55–68, 1992.
- 953 **13** Ryan R Curtin, Dongryeol Lee, William B March, and Parikshit Ram. Plug-and-play dual-tree
954 algorithm runtime analysis. *J. Mach. Learn. Res.*, 16:3269–3297, 2015.
- 955 **14** William IF David, Kenneth Shankland, Ch Baerlocher, LB McCusker, et al. *Structure*
956 *determination from powder diffraction data*, volume 13. 2002.
- 957 **15** N Dolbilin and M Bouniaev. Regular t -bonded systems in \mathbb{R}^3 . *European Journal of Combinat-*
958 *orics*, 80:89–101, 2019.

- 959 16 N. Dolbilin, J Lagarias, and M. Senechal. Multiregular point systems. *Discrete & Computational*
960 *Geometry*, 20(4):477–498, 1998.
- 961 17 Nadav Dym and Shahar Ziv Kovalsky. Linearly converging quasi branch and bound algorithms
962 for global rigid registration. In *Proceedings of the IEEE/CVF International Conference on*
963 *Computer Vision*, pages 1628–1636, 2019.
- 964 18 Herbert Edelsbrunner, Teresa Heiss, Vitaliy Kurlin, Philip Smith, and Mathijs Wintraecken.
965 The density fingerprint of a periodic point set. In *Proceedings of SoCG*, 2021.
- 966 19 Yury Elkin. New geometric methods for a data-led discovery of topological shapes (phd thesis
967 at the university of liverpool), 2021.
- 968 20 Giuseppe Fadda and Giovanni Zanzotto. On the arithmetic classification of crystal structures.
969 *Acta Cryst. A: Foundations*, 57(5):492–506, 2001.
- 970 21 Cosmin Grigorescu and Nicolai Petkov. Distance sets for shape filters and shape recognition.
971 *IEEE transactions on image processing*, 12(10):1274–1286, 2003.
- 972 22 F Grünbaum and C Moore. The use of higher-order invariants in the determination of
973 generalized Patterson cyclotomic sets. *Acta Crystallographica Section A*, 51:310–323, 1995.
- 974 23 T Hahn, U Shmueli, and J Arthur. *Internat. tables for crystallography*, volume 1. 1983.
- 975 24 Heuna Kim and Günter Rote. Congruence testing of point sets in 4 dimensions.
976 *arXiv:1603.07269*, 2016.
- 977 25 Leo Liberti and Carlile Lavor. *Euclidean distance geometry*. Springer, 2017.
- 978 26 Siddharth Manay, Daniel Cremers, Byung-Woo Hong, Anthony J Yezzi, and Stefano Soatto.
979 Integral invariants for shape matching. *Transactions PAMI*, 28(10):1602–1618, 2006.
- 980 27 Haggai Maron, Nadav Dym, Itay Kezurer, Shahar Kovalsky, and Yaron Lipman. Point
981 registration via efficient convex relaxation. *ACM Trans. on Graphics*, 35(4):1–12, 2016.
- 982 28 Leland McInnes, John Healy, and James Melville. Umap: Uniform manifold approximation
983 and projection for dimension reduction. *arXiv:1802.03426*, 2018.
- 984 29 Facundo Mémoli. Gromov–wasserstein distances and the metric approach to object matching.
985 *Foundations of computational mathematics*, 11(4):417–487, 2011.
- 986 30 Robert Osada, Thomas Funkhouser, Bernard Chazelle, and David Dobkin. Shape distributions.
987 *ACM Transactions on Graphics (TOG)*, 21(4):807–832, 2002.
- 988 31 A Patterson. Ambiguities in the x-ray analysis of structures. *Phys. Rev.*, 65:195–201, 1944.
- 989 32 Helmut Pottmann, Johannes Wallner, Qi-Xing Huang, and Yong-Liang Yang. Integral
990 invariants for robust geometry processing. *Comp. Aided Geom. Design*, 26(1):37–60, 2009.
- 991 33 S Pozdnyakov, M Willatt, A Bartók, C Ortner, G Csányi, and M Ceriotti. Incompleteness of
992 atomic structure representations. *Phys. Rev. Lett.*, 125:166001, 2020. URL: [arXiv:2001.11696](https://arxiv.org/abs/2001.11696).
- 993 34 Daniel Probst and Jean-Louis Reymond. Visualization of very large high-dimensional data
994 sets as minimum spanning trees. *Cheminformatics*, 12:1–13, 2020.
- 995 35 A Pulido, L Chen, T Kaczorowski, D Holden, M Little, S Chong, B Slater, D McMahon,
996 B Bonillo, C Stackhouse, A Stephenson, C Kane, R Clowes, T Hasell, A Cooper, and G Day.
997 Functional materials discovery using energy–structure maps. *Nature*, 543:657–664, 2017.
- 998 36 Joseph Rosenblatt and Paul D Seymour. The structure of homometric sets. *SIAM Journal on*
999 *Algebraic Discrete Methods*, 3(3):343–350, 1982.
- 1000 37 Y. Rubner, C. Tomasi, and L. Guibas. The earth mover’s distance as a metric for image
1001 retrieval. *Intern. Journal of Computer Vision*, 40(2):99–121, 2000.
- 1002 38 Mauro R Ruggeri and Dietmar Saupe. Isometry-invariant matching of point set surfaces. In
1003 *3DOR*, pages 17–24. Citeseer, 2008.
- 1004 39 Ryoma Sato, Marco Cuturi, Makoto Yamada, and Hisashi Kashima. Fast and robust comparison
1005 of probability measures in heterogeneous spaces. *arXiv:2002.01615*, 2020.
- 1006 40 Nino Shervashidze, Pascal Schweitzer, Erik Jan Van Leeuwen, Kurt Mehlhorn, and Karsten M
1007 Borgwardt. Weisfeiler-lehman graph kernels. *J. Machine Learning Research*, 12(9), 2011.
- 1008 41 Sameer Shirdhonkar and David W Jacobs. Approximate earth mover’s distance in linear time.
1009 In *Conference on Computer Vision and Pattern Recognition*, pages 1–8, 2008.

- 1010 42 Laurens Van der Maaten and Geoffrey Hinton. Visualizing data using t-sne. *Journal of*
1011 *machine learning research*, 9(11), 2008.
- 1012 43 Daniel Widdowson, Marco Mosca, Angeles Pulido, Vitaliy Kurlin, and Andrew Cooper. Average
1013 minimum distances of periodic point sets. *MATCH Communications in Mathematical and in*
1014 *Computer Chemistry*, to appear. URL: <https://arxiv.org/abs/2009.02488>.
- 1015 44 Jiaolong Yang, Hongdong Li, Dylan Campbell, and Yunde Jia. Go-icp: A globally optimal
1016 solution to 3d icp point-set registration. *IEEE transactions on pattern analysis and machine*
1017 *intelligence*, 38(11):2241–2254, 2015.
- 1018 45 B. Zhilinskii. *Introduction to lattice geometry through group action*. EDP sciences, 2016.
- 1019 46 Peter Zwart, Ralf Grosse-Kunstleve, Andrey Lebedev, Garib Murshudov, and Paul Adams.
1020 Surprises and pitfalls arising from (pseudo) symmetry. *Acta Cryst. D*, 64:99–107, 2008.